ISSN 1063-7788, Physics of Atomic Nuclei, 2014, Vol. 77, No. 3, pp. 389–413. © Pleiades Publishing, Ltd., 2014.

NUCLEI
Theory

Resonant Tunneling of a Few-Body Cluster Through Repulsive Barriers*

A. A. Gusev[1)**], S. I. Vinitsky[1)], O. Chuluunbaatar[1),2)], L. L. Hai[1)], V. L. Derbov[3)], A. Góźdź[4)], and P. M. Krassovitskiy[5)]

Received April 18, 2013

Abstract—A model for quantum tunnelling of a cluster comprised of A identical particles, interacting via oscillator-type potential, through short-range repulsive barrier potentials is introduced for the first time in symmetrized-coordinate representation and numerically studied in the s-wave approximation. A constructive method for symmetrizing or antisymmetrizing the $(A-1)$-dimensional harmonic oscillator basis functions in the new symmetrized coordinates with respect to permutations of coordinates of A identical particles is described. The effect of quantum transparency, manifesting itself in nonmonotonic resonance-type dependence of the transmission coefficient upon the energy of the particles, their number $A = 2, 3, 4$ and the type of their symmetry, is analyzed. It is shown that the total transmission coefficient demonstrates the resonance behavior due to the existence of barrier quasi-stationary states, embedded in the continuum.

DOI: 10.1134/S1063778814030107

1. INTRODUCTION

During a decade the mechanism of quantum penetration of two bound particles through repulsive barriers, manifested in [1], attracts attention from both theoretical and experimental viewpoints in relation with such problems as near-surface quantum diffusion of molecules [2–5], fragmentation in producing very neutron-rich light nuclei [6–9], and heavy-ion collisions through multidimensional barriers [10–16]. In a general formulation of the scattering problem for ions having different masses a benchmark model with long-range potentials was proposed in [17, 18]. The generalization of the two-particle model over a quantum system of A identical particles is of great importance for appropriate description of molecular and heavy-ion collisions as well as a microscopic study of tetrahedral-symmetric nuclei [19, 20]. *The aim of this paper is to present a suitable formulation of the problem stated above and calculation methods for solving it.*

We consider the penetration of A identical quantum particles, coupled by short-range oscillator-like interaction, through a repulsive potential barrier. We assume that the spin part of the wave function is known, so that only the spatial part of the wave function is to be considered, which may be symmetric or antisymmetric with respect to a permutation of A identical particles [21–24]. The initial problem is reduced to penetration of a composite system with the internal degrees of freedom, describing an $(A-1)\times d$-dimensional oscillator, and the external degrees of freedom, describing the center-of-mass motion of A particles in d-dimensional Euclidean space. For simplicity, we restrict our consideration to the so-called s-wave approximation [1], corresponding to one-dimensional Euclidean space ($d = 1$). It is shown that the reduction is provided by using appropriately chosen symmetrized coordinates, rather than the conventional Jacoby coordinates. The main goal of introducing the symmetrized coordinates is to provide invariance of the Hamiltonian with respect to permutations of A identical particles. This allows construction not only of basis functions, symmetric or antisymmetric under permutations of $A-1$ relative coordinates, but also of basis functions, symmetric (S) or antisymmetric (A) under permutations of A Cartesian coordinates. We refer the expansion of the solution in the basis of such type as symmetrized coordinate representation (SCR).

We seek for the solution in the form of Galerkin or Kantorovich expansions [25] with unknown coefficients having the form of matrix functions of the center-of-mass variables in the SCR. As a result, the problem is reduced to a boundary-value problem for a

*The text was submitted by the authors in English.

1)Joint Institute for Nuclear Research, Dubna, Russia.
2) National University of Mongolia, Ulaanbaatar.
3)Saratov State University, Russia.
4)Department of Mathematical Physics, Institute of Physics, University of Maria Curie–Skłodowska, Lublin, Poland.
5)Institute of Nuclear Physics, Almaty, Kazakhstan.
**E-mail: gooseff@jinr.ru

system of ordinary second-order differential equations with respect to the center-of-mass variable. Conventional asymptotic boundary conditions are imposed on the desired matrix solution. The results of calculations are analyzed with particular emphasis on the effect of quantum transparency that manifests itself as nonmonotonic energy dependence of the transmission coefficient due to resonance tunnelling of the bound particles in S (A) states through the repulsive potential barriers.

The paper is organized as follows. In Section 2 we present the statement of the problem in conventional Jacobi and symmetrized coordinates. In Section 3 we introduce the SCR of the solution of the considered problem. In Section 4 we formulate the boundary-value problem for close-coupling equations in Galerkin and Kantorovich forms using conventional and parametric SCRs, respectively. In Section 5 we analyze the results of a numerical experiment on resonance transmission of a few coupled identical particles in S (A) states. In Conclusion we sum up the results and discuss briefly the perspectives of application of the developed approach.

2. THE STATEMENT OF THE PROBLEM

The problem of penetration of A identical quantum particles with the mass m and a set of the Cartesian coordinates $x_i \in \mathbf{R}^d$ in d-dimensional Euclidean space, considered as vector $\tilde{\mathbf{x}} = (\tilde{x}_1, \ldots, \tilde{x}_A) \in \mathbf{R}^{A\times d}$ in $A \times d$-dimensional configuration space, coupled by the pair potential $\tilde{V}^{\text{pair}}(\tilde{x}_{ij})$ of relative coordinates, $\tilde{x}_{ij} = \tilde{x}_i - \tilde{x}_j$, similar to a harmonic oscillator $\tilde{V}^{\text{hosc}}(\tilde{x}_{ij}) = \frac{m\omega^2}{2}(\tilde{x}_{ij})^2$ with frequency ω, through the repulsive potential barriers $\tilde{V}(\tilde{x}_i)$ is described by the Schrödinger equation

$$\left[-\frac{\hbar^2}{2m}\sum_{i=1}^{A}\frac{\partial^2}{\partial\tilde{x}_i^2} + \sum_{i,j=1;i<j}^{A}\tilde{V}^{\text{pair}}(\tilde{x}_{ij}) + \sum_{i=1}^{A}\tilde{V}(\tilde{x}_i) - \tilde{E}\right]\tilde{\Psi}(\tilde{x}_1,\ldots,\tilde{x}_A) = 0,$$

where $\tilde{E}$ is the total energy of the system of A particles and $\tilde{P}^2 = 2m\tilde{E}/\hbar^2$, $\tilde{P}$ is the total momentum of the system of A particles. Using the oscillator units $x_{\text{osc}} = \sqrt{\hbar/(m\omega\sqrt{A})}$, $p_{\text{osc}} = \sqrt{(m\omega\sqrt{A})/\hbar} = x_{\text{osc}}^{-1}$, and $E_{\text{osc}} = \hbar\omega\sqrt{A}/2$ to introduce the dimensionless coordinates $x_i = \tilde{x}_i/x_{\text{osc}}$, $x_{ij} = \tilde{x}_{ij}/x_{\text{osc}} = x_i - x_j$, $E = \tilde{E}/E_{\text{osc}} = P^2$, $P = \tilde{P}/p_{\text{osc}} = \tilde{P}x_{\text{osc}}$, $V^{\text{pair}}(x_{ij}) = \tilde{V}^{\text{pair}}(x_{ij}x_{\text{osc}})/E_{\text{osc}}$, $V^{\text{hosc}}(x_{ij}) = \tilde{V}^{\text{hosc}}(x_{ij}x_{\text{osc}})/E_{\text{osc}} = \frac{1}{A}(x_{ij})^2$, and $V(x_i) = \tilde{V}(x_ix_{\text{osc}})/E_{\text{osc}}$, one can rewrite the above equation in the form

$$\left[-\sum_{i=1}^{A}\frac{\partial^2}{\partial x_i^2} + \sum_{i,j=1;i<j}^{A}\frac{1}{A}(x_{ij})^2 + \sum_{i,j=1;i<j}^{A}U^{\text{pair}}(x_{ij}) + \sum_{i=1}^{A}V(x_i) - E\right] \times \Psi(x_1,\ldots,x_A) = 0, \quad (1)$$

where $U^{\text{pair}}(x_{ij}) = V^{\text{pair}}(x_{ij}) - V^{\text{hosc}}(x_{ij})$, i.e., if $V^{\text{pair}}(x_{ij}) = V^{\text{hosc}}(x_{ij})$, then $U^{\text{pair}}(x_{ij}) = 0$.

Our goal is to find the solutions $\Psi(x_1,\ldots,x_A)$ of Eq. (1), totally symmetric (or antisymmetric) with respect to the permutations of A particles that belong to the permutation group S_n. The permutation of particles is nothing but a permutation of the Cartesian coordinates $x_i \leftrightarrow x_j$, $i,j = 1,\ldots,A$.

First, we introduce the Jacobi coordinates following one of the possible definitions [7]

$$y_0 = \frac{1}{\sqrt{A}}\left(\sum_{t=1}^{A}x_t\right), \quad (2)$$

$$y_s = \frac{1}{\sqrt{s(s+1)}}\left(\sum_{t=1}^{s}x_t - sx_{s+1}\right), \quad s = 1,\ldots,A-1.$$

In the matrix form Eqs. (2) read as

$$\begin{pmatrix} y_0\\ y_1\\ y_2\\ y_3\\ \vdots\\ y_{A-1}\end{pmatrix} = J\begin{pmatrix} x_1\\ x_2\\ x_3\\ \vdots\\ x_{A-1}\\ x_A\end{pmatrix}, \quad J = \begin{pmatrix} 1/\sqrt{A} & 1/\sqrt{A} & 1/\sqrt{A} & 1/\sqrt{A} & \cdots & 1/\sqrt{A}\\ 1/\sqrt{2} & -1/\sqrt{2} & 0 & 0 & \cdots & 0\\ 1/\sqrt{6} & 1/\sqrt{6} & -2/\sqrt{6} & 0 & \cdots & 0\\ 1/\sqrt{12} & 1/\sqrt{12} & 1/\sqrt{12} & -3/\sqrt{12} & \cdots & 0\\ \vdots & \vdots & \vdots & \vdots & \ddots & \vdots\\ \frac{1}{\sqrt{(A-1)A}} & \frac{1}{\sqrt{(A-1)A}} & \frac{1}{\sqrt{(A-1)A}} & \frac{1}{\sqrt{(A-1)A}} & \cdots & -\frac{A-1}{\sqrt{(A-1)A}}\end{pmatrix}.$$

The inverse coordinate transformation is implemented using the transposed matrix $J^{-1} = J^T$, i.e. J is an orthogonal matrix with pairs of complex conjugate eigenvalues, the absolute values of which are equal to one.

The Jacobi coordinates have the property $\sum_{i=0}^{A-1}(y_i \cdot y_i) = \sum_{i=1}^{A}(x_i \cdot x_i) = r^2$. Consequently,

$$\sum_{i,j=1}^{A}(x_{ij})^2 = 2A\sum_{i=0}^{A-1}(y_i)^2$$
$$-2\left(\sum_{i=1}^{A}x_i\right)^2 = 2A\sum_{i=1}^{A-1}(y_i)^2,$$

so that Eq. (1) takes the form

$$\left[-\frac{\partial^2}{\partial y_0^2} + \sum_{i=1}^{A-1}\left(-\frac{\partial^2}{\partial y_i^2} + (y_i)^2\right)\right.$$
$$\left. + U(y_0,\ldots,y_{A-1}) - E\right]\Psi(y_0,\ldots,y_{A-1}) = 0,$$
$$U(y_0,\ldots,y_{A-1})$$
$$= \sum_{i,j=1;i<j}^{A} U^{\text{pair}}(x_{ij}(y_1,\ldots,y_{A-1}))$$
$$+ \sum_{i=1}^{A} V(x_i(y_0,\ldots,y_{A-1})),$$

which, as follows from Eq. (2), is *not invariant* with respect to permutations $y_i \leftrightarrow y_j$ at $i,j = 1,\ldots,A-1$.

The construction of desirable solutions of Eq. (1) in the form of linear combinations of the solutions of Eq. (3), totally symmetric (antisymmetric) with respect to permutations of coordinates $x_i \leftrightarrow x_j$ (at $i,j = 1,\ldots,A$) of A identical particles is implemented using various special procedures (see, e.g., [26–35]).

Symmetrized Coordinates

As will be shown below, a simple and clear way to construct the states keeping the symmetry (antisymmetry) under the permutations of A initial Cartesian coordinates, which we refer as S (A) states, is to use the symmetrized relative coordinates rather than the Jacobi coordinates.

The transformation from the Cartesian coordinates to one of the possible choices of symmetrized ones ξ_i has the form:

$$\xi_0 = \frac{1}{\sqrt{A}}\left(\sum_{t=1}^{A}x_t\right), \qquad (3)$$

$$\xi_s = \frac{1}{\sqrt{A}}\left(x_1 + \sum_{t=2}^{A}a_0 x_t + \sqrt{A}x_{s+1}\right),$$
$$s = 1,\ldots,A-1,$$
$$x_1 = \frac{1}{\sqrt{A}}\left(\sum_{t=0}^{A-1}\xi_t\right),$$
$$x_s = \frac{1}{\sqrt{A}}\left(\xi_0 + \sum_{t=1}^{A-1}a_0\xi_t + \sqrt{A}\xi_{s-1}\right),$$
$$s = 2,\ldots,A,$$

or, in the matrix form,

$$\begin{pmatrix}\xi_0\\ \xi_1\\ \xi_2\\ \vdots\\ \xi_{A-2}\\ \xi_{A-1}\end{pmatrix} = C\begin{pmatrix}x_1\\ x_2\\ x_3\\ \vdots\\ x_{A-1}\\ x_A\end{pmatrix}, \qquad (4)$$

$$\begin{pmatrix}x_1\\ x_2\\ x_3\\ \vdots\\ x_{A-1}\\ x_A\end{pmatrix} = C^{-1}\begin{pmatrix}\xi_0\\ \xi_1\\ \xi_2\\ \vdots\\ \xi_{A-2}\\ \xi_{A-1}\end{pmatrix},$$

$$C = \frac{1}{\sqrt{A}}\begin{pmatrix}1 & 1 & 1 & 1 & \cdots & 1 & 1\\ 1 & a_1 & a_0 & a_0 & \cdots & a_0 & a_0\\ 1 & a_0 & a_1 & a_0 & \cdots & a_0 & a_0\\ 1 & a_0 & a_0 & a_1 & \cdots & a_0 & a_0\\ \vdots & \vdots & \vdots & \vdots & \ddots & \vdots & \vdots\\ 1 & a_0 & a_0 & a_0 & \cdots & a_1 & a_0\\ 1 & a_0 & a_0 & a_0 & \cdots & a_0 & a_1\end{pmatrix},$$

where $a_0 = 1/(1-\sqrt{A}) < 0$, $a_1 = a_0 + \sqrt{A}$. The inverse coordinate transformation is performed using the same matrix $C^{-1} = C$, $C^2 = I$, i.e. $C = C^T$ is a symmetric orthogonal matrix with the eigenvalues $\lambda_1 = -1$, $\lambda_2 = 1$, …, $\lambda_A = 1$ and $\det C = -1$. At $A = 2$ the symmetrized variables (4) are similar up to normalization factors to the symmetrized Jacobi coordinates (2) considered in [36], while at $A = 4$ they correspond to another choice of symmetrized co-

ordinates $(\ddot{x}_4, \ddot{x}_1, \ddot{x}_2, \ddot{x}_3)^T = C(x_4, x_1, x_2, x_3)^T$ considered in [26, 37], and mentioned earlier in [38]. We could not find a general definition of symmetrized coordinates for A identical particles like (4) in the available literature, so we believe that in the present paper it is introduced for the first time.

With the relations $a_1 - a_0 = \sqrt{A}$, $a_0 - 1 = a_0\sqrt{A}$ taken into account, the relative coordinates $x_{ij} \equiv x_i - x_j$ of a pair of particles i and j are expressed in terms of the internal $A-1$ symmetrized coordinates only:

$$x_{ij} \equiv x_i - x_j = \xi_{i-1} - \xi_{j-1} \equiv \xi_{i-1,j-1}, \quad (5)$$
$$x_{i1} \equiv x_i - x_1 = \xi_{i-1} + a_0 \sum_{i'=1}^{A-1} \xi_{i'},$$
$$i, j = 2, \ldots, A.$$

So, if only the absolute values of x_{ij} are to be considered, then there are $(A-1)(A-2)/2$ old relative coordinates transformed into new relative ones and $A-1$ old relative coordinates expressed in terms of $A-1$ internal symmetrized coordinates. These important relations essentially simplify the procedures of symmetrization (or antisymmetrization) of the oscillator basis functions and the calculations of the corresponding pair-interaction integrals $V^{\text{pair}}(x_{ij})$. Note that the symmetrized coordinates are related with the Jacobi ones as

$$\begin{pmatrix} y_0 \\ y_1 \\ y_2 \\ \vdots \\ y_{A-2} \\ y_{A-1} \end{pmatrix} = B \begin{pmatrix} \xi_0 \\ \xi_1 \\ \xi_2 \\ \vdots \\ \xi_{A-2} \\ \xi_{A-1} \end{pmatrix}, \quad B = JC$$

$$= \begin{pmatrix} 1 & 0 & 0 & 0 & 0 & \cdots & 0 & 0 \\ 0 & b_1^0 & b_1^- & b_1^- & b_1^- & \cdots & b_1^- & b_1^- \\ 0 & b_2^+ & b_2^0 & b_2^- & b_2^- & \cdots & b_2^- & b_2^- \\ 0 & b_3^+ & b_3^+ & b_3^0 & b_3^- & \cdots & b_3^- & b_3^- \\ 0 & b_4^+ & b_4^+ & b_4^+ & b_4^0 & \cdots & b_4^- & b_4^- \\ \vdots & \vdots & \vdots & \vdots & \vdots & \ddots & \vdots & \vdots \\ 0 & b_{A-1}^+ & b_{A-1}^+ & b_{A-1}^+ & b_{A-1}^+ & \cdots & b_{A-1}^+ & b_{A-1}^0 \end{pmatrix},$$

where $b_s^+ = 1/((\sqrt{A}-1)\sqrt{s(s+1)})$, $b_s^- = \sqrt{A}/((\sqrt{A}-1)\sqrt{s(s+1)})$, and $b_s^0 = (1+s-s\sqrt{A})/((\sqrt{A}-1)\sqrt{s(s+1)})$. One can see that for the center of mass the symmetrized and Jacobi coordinates are equal, $y_0 = \xi_0$, while the relative coordinates are related via the $(A-1)\times(A-1)$ matrix M with the elements $M_{ij} = B_{i+1,j+1}$ and $\det M = (-1)^{A\times d}$, i.e. the matrix, obtained by cancelling the first row and the first column. The inverse transformation is given by the matrix $B^{-1} = (JC)^{-1} = CJ^T = B^T$, i.e., B is also an orthogonal matrix.

Note, that for $A = 3$ and $d = 1$ the relation between the Jacobi coordinates

$$y_1 = 1/\sqrt{2}(x_1 - x_2), \quad y_2 = 1/\sqrt{6}(x_1 + x_2 - 2x_3)$$

and the symmetrized ones

$$\xi_1 = 1/\sqrt{3}(x_1 + 1/2(\sqrt{3}-1)x_2 - 1/2(\sqrt{3}+1)x_3),$$
$$\xi_2 = 1/\sqrt{3}(x_1 - 1/2(\sqrt{3}+1)x_2 + 1/2(\sqrt{3}-1)x_3)$$

is given by the orthogonal matrix M:

$$M = \begin{pmatrix} b_1^0 & b_1^- \\ b_2^+ & b_2^0 \end{pmatrix} \quad (6)$$
$$= \begin{pmatrix} (\sqrt{6}-\sqrt{2})/4 & (\sqrt{6}+\sqrt{2})/4 \\ (\sqrt{6}+\sqrt{2})/4 & -(\sqrt{6}-\sqrt{2})/4 \end{pmatrix}$$
$$= \begin{pmatrix} \sin\phi_1 & \cos\phi_1 \\ \cos\phi_1 & -\sin\phi_1 \end{pmatrix}$$
$$= \begin{pmatrix} 0 & 1 \\ 1 & 0 \end{pmatrix} \begin{pmatrix} \cos\phi_1 & -\sin\phi_1 \\ \sin\phi_1 & \cos\phi_1 \end{pmatrix}$$
$$= \begin{pmatrix} \cos\phi_1 & \sin\phi_1 \\ -\sin\phi_1 & \cos\phi_1 \end{pmatrix} \begin{pmatrix} 0 & 1 \\ 1 & 0 \end{pmatrix}$$
$$= M_1(\phi_1) M_0.$$

This transformation is a product of the permutation of coordinates $(\xi_1, \xi_2) \to (\xi_2, \xi_1)$ and the counterclockwise rotation by the angle $\phi_1 = \pi/12$. A schematic 3D image in the left panel of Fig. 1 shows the coordinate planes (marked with 1, 2, 3) and the center-of-mass plane in $\mathbf{R}^3$ (its visible part having the shape of a hexagon), together with the lines of intersection of these planes with pair-collision planes ($x_i = x_j$), which correspond to pair-collision lines ($\{x_i = x_j, x_1 + x_2 + x_3 = 0\}$) (marked with 12, 23, 13) in the center-of-mass plane $x_1 + x_2 + x_3 = 0$, belonging to $\mathbf{R}^2$. Different projections of this geometry clarify the nature of the Jacobi (y_1, y_2) and the symmetric (ξ_1, ξ_2) coordinates (middle and right

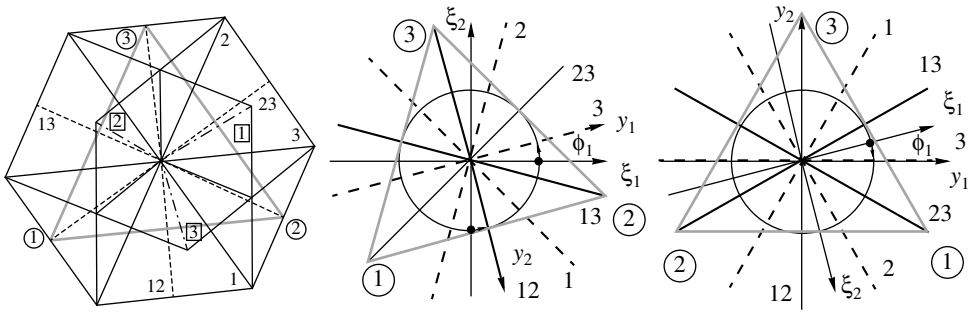

Fig. 1. (Left panel) The coordinate planes 1, 2, 3, labelled with boxes, the center-of-mass plane in $\mathbf{R}^3$, and the lines of intersection of these planes with the pair-collision planes $x_i = x_j$, corresponding to pair-collision lines $\{x_i = x_j, x_1 + x_2 + x_3 = 0\}$ (labelled 12, 23, 13) in the center-of-mass plane $x_1 + x_2 + x_3 = 0$, belonging to $\mathbf{R}^2$. (Middle and right panels) The equilateral triangle showing the isomorphism between the group of its symmetry operations D_3 in $\mathbf{R}^2$ and the group of permutations S_3 of three objects 1, 2, 3, labelled with circles. The symmetric (ξ_1, ξ_2) and Jacobi (y_1, y_2) coordinates, related via the transformation (6) in the center-of-mass plane $\mathbf{R}^2$, respectively.

panels, respectively), related by the above transformation in the center-of-mass plane $\mathbf{R}^2$. This illustrates the isomorphism between the symmetry group of an equilateral triangle D_3 in $\mathbf{R}^2$ and the 3-body permutation group S_3 ($A = 3$), discussed in [34, 39, 40] in a different context.

At $A = 4$ and $d = 1$ the relation between the Jacobi coordinates

$$y_1 = 1/\sqrt{2}(x_1 - x_2),$$
$$y_2 = 1/\sqrt{6}(x_1 + x_2 - 2x_3),$$
$$y_3 = 1/\sqrt{12}(x_1 + x_2 + x_3 - 3x_4)$$

and the symmetrized ones

$$\xi_1 = 1/2(x_1 + x_2 - x_3 - x_4),$$
$$\xi_2 = 1/2(x_1 - x_2 + x_3 - x_4),$$
$$\xi_3 = 1/2(x_1 - x_2 - x_3 + x_4)$$

is given by the orthogonal matrix M:

$$M = \begin{pmatrix} b_1^0 & b_1^- & b_1^- \\ b_2^+ & b_2^0 & b_2^- \\ b_3^+ & b_3^+ & b_3^0 \end{pmatrix}$$

$$= \begin{pmatrix} 0 & \sqrt{2}/2 & \sqrt{2}/2 \\ \sqrt{6}/3 & -\sqrt{6}/6 & \sqrt{6}/6 \\ \sqrt{3}/3 & \sqrt{3}/3 & -\sqrt{3}/3 \end{pmatrix}.$$

One of the possible decompositions $M = M_3(\phi_3) \times M_2(\phi_2)M_1(\phi_1)$ of this matrix is

$$M = \begin{pmatrix} 1 & 0 & 0 \\ 0 & \cos\phi_3 & \sin\phi_3 \\ 0 & -\sin\phi_3 & \cos\phi_3 \end{pmatrix} \qquad (7)$$

$$\times \begin{pmatrix} \cos\phi_2 & \sin\phi_2 & 0 \\ -\sin\phi_2 & \cos\phi_2 & 0 \\ 0 & 0 & 1 \end{pmatrix} \begin{pmatrix} 1 & 0 & 0 \\ 0 & \cos\phi_1 & \sin\phi_1 \\ 0 & -\sin\phi_1 & \cos\phi_1 \end{pmatrix}.$$

This transformation is a product of three counterclockwise rotations: the first of them by the angle $\phi_1 = 3\pi/4$ about the first old axis, the second one by the angle $\phi_2 = \pi - \arctan(\sqrt{2}) \approx 16\pi/23$ about the third new axis, and the third one by the angle $\phi_3 = \pi/3$ about the first new axis. Note, that the second angle ϕ_2 is supplementary to the angle between an edge and a face of a regular tetrahedron, associated with the system of symmetrized coordinates $\{\xi_1, \xi_2, \xi_3\} \in \mathbf{R}^3$. This transformation illustrates the isomorphism between the tetrahedron group T_d in $\mathbf{R}^3$ and the 4-particle permutation group S_4 ($A = 4$), discussed in [26] in the case of $d = 3$. The three transformations $M = M_3(\phi_3)M_2(\phi_2)M_1(\phi_1)$ are illustrated in Fig. 2.

Note, that the transformations from the initial coordinates to Jacobi coordinates are rotations in $A \times d$-configuration space, while the transformations from the initial coordinates to the symmetrized ones involve also permutations or reflections. The transformations between Jacobi and symmetrized coordinates in the center-of-mass hyperplane are rotations in the $(A-1) \times d$-configuration space, but for odd $A \times d$ they involve also a permutation or reflection. The key point of using the symmetrized coordinates is that in these coordinates the symmetry with respect to a permutation of two identical particles coincides with the symmetry with respect to a geometrical reflection in the $(A-2) \times d$-dimensional plane $\xi_i - \xi_j = 0$. For example, at $A = 3$ and $d = 1$, such $((A-2) \times d = 1)$-dimensional objects are lines $\xi_i - \xi_j = 0$, see Fig. 1, while at $A = 4$ and $d = 1$, such $((A-$

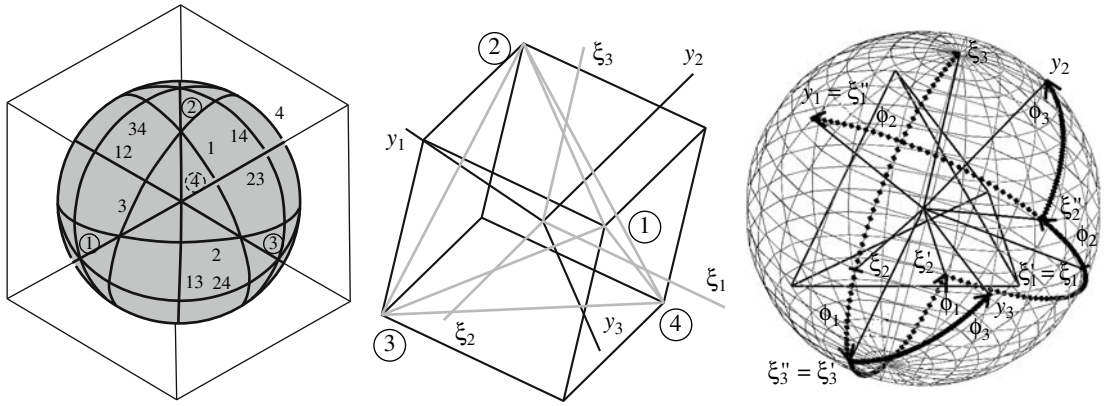

Fig. 2. (Left panel) Intersections in $\mathbf{R}^4$ of the coordinate spaces $\mathbf{R}^3$ (labelled 1, 2, 3, 4) and the spaces $\mathbf{R}^3$ of pair collisions (labelled 12, etc.) with the sphere $\mathbf{S}^2$ in the center-of-mass space $\mathbf{R}^3$. (Middle and right panels) The tetrahedron showing the isomorphism between the group of its symmetry operations T_d in $\mathbf{R}^3$ and the group of permutations S_4 of four objects 1, 2, 3, 4, labelled with circles. The two systems of coordinates, (y_1, y_2, y_3) and (ξ_1, ξ_2, ξ_3), are related via the transformation (7), i.e. via three counterclockwise rotations by the angles $\phi_1 = 3\pi/4$, $\phi_2 = \pi - \arctan\sqrt{2}$, and $\phi_3 = \pi/3$ about the axes ξ_1, ξ_3', and $y_1 = \xi_1''$, respectively, are used in the text.

$2) \times d = 2)$-dimensional objects are 2D planes. The lines in $\mathbf{R}^4$, corresponding to the intersection of the coordinate spaces $\mathbf{R}^3$ (labelled 1, 2, 3, 4) and the pair-collision spaces $\mathbf{R}^3$ (labelled 12, etc.) with the sphere $\mathbf{S}^2$ in the center-of-mass space $\mathbf{R}^3$ are shown in Fig. 2.

In the symmetrized coordinates Eq. (1) takes the form

$$\left[-\frac{\partial^2}{\partial \xi_0^2} + \sum_{i=1}^{A-1} \left(-\frac{\partial^2}{\partial \xi_i^2} + (\xi_i)^2 \right) + U(\xi_0, \ldots, \xi_{A-1}) - E \right] \Psi(\xi_0, \ldots, \xi_{A-1}) = 0, \tag{8}$$

$$U(\xi_0, \ldots, \xi_{A-1}) = \sum_{i,j=1; i<j}^{A} U^{\text{pair}}(x_{ij}(\xi_1, \ldots, \xi_{A-1})) + \sum_{i=1}^{A} V(x_i(\xi_0, \ldots, \xi_{A-1})),$$

which is *invariant* under permutations $\xi_i \leftrightarrow \xi_j$ at $i, j = 1, \ldots, A-1$, as follows from Eq. (4), i.e., the *invariance* of Eq. (1) under permutations $x_i \leftrightarrow x_j$ at $i, j = 1, \ldots, A$ survives. This remarkable fact is one of the most prominent features of the proposed approach.

Here and below we use the oscillator units introduced above.

Asymptotic Boundary Conditions

For simplicity we restrict our consideration to the so-called s-wave approximation [1], i.e., one-dimensional Euclidean space ($d = 1$). The asymptotic boundary conditions for the solution $\Psi(\xi_0, \boldsymbol{\xi}) = \{\Psi_{i_o}(\xi_0, \boldsymbol{\xi})\}_{i_o=1}^{N_o}$ (ξ_0, $\boldsymbol{\xi} = \{\xi_1, \ldots, \xi_{A-1}\}$) have the form

$$\Psi_{i_o}^{\leftrightarrows}(\xi_0 \to \pm\infty, \boldsymbol{\xi}) \to \tilde{\Phi}_{i_o}(\boldsymbol{\xi}) \frac{\exp(\mp\imath(p_{i_o}\xi_0))}{\sqrt{p_{i_o}}} + \sum_{j=1}^{N_o} \tilde{\Phi}_j(\boldsymbol{\xi}) \frac{\exp(\pm\imath(p_j\xi_0))}{\sqrt{p_j}} R_{ji_o}^{\leftrightarrows}(E),$$

$$\Psi_{i_o}^{\leftrightarrows}(\xi_0 \to \mp\infty, \boldsymbol{\xi}) \to \sum_{j=1}^{N_o} \tilde{\Phi}_j(\boldsymbol{\xi}) \frac{\exp(\mp\imath(p_j\xi_0))}{\sqrt{p_j}} T_{ji_o}^{\leftrightarrows}(E),$$

$$\Psi_{i_o}^{\leftrightarrows}(\xi_0, |\boldsymbol{\xi}| \to \infty) \to 0. \tag{9}$$

Here, $v = \leftarrow, \rightarrow$ indicates the initial direction of the particle motion along the ξ_0 axis, N_o is the number of open channels at the fixed energy E and relative momentum $p_{i_o}^2 = E - E_{i_o} > 0$ of the cluster; $R_{ji_o}^{\leftarrow} = R_{ji_o}^{\leftarrow}(E)$, $R_{ji_o}^{\rightarrow} = R_{ji_o}^{\rightarrow}(E)$ and $T_{ji_o}^{\leftarrow} = T_{ji_o}^{\leftarrow}(E)$, $T_{ji_o}^{\rightarrow} = T_{ji_o}^{\rightarrow}(E)$ are unknown amplitudes of the reflected and transmitted waves. We can rewrite Eqs. (9) in the matrix form $\boldsymbol{\Psi} = \boldsymbol{\Phi}^T \mathbf{F}$, describing the incident wave and outgoing waves at $\xi_0^+ \to +\infty$ and $\xi_0^- \to -\infty$ as

$$\begin{pmatrix} \mathbf{F}_{\rightarrow}(\xi_0^+) & \mathbf{F}_{\leftarrow}(\xi_0^+) \\ \mathbf{F}_{\rightarrow}(\xi_0^-) & \mathbf{F}_{\leftarrow}(\xi_0^-) \end{pmatrix} \tag{10}$$

$$= \begin{pmatrix} \mathbf{0} & \mathbf{X}^{(-)}(\xi_0^+) \\ \mathbf{X}^{(+)}(\xi_0^-) & \mathbf{0} \end{pmatrix} + \begin{pmatrix} \mathbf{0} & \mathbf{X}^{(+)}(\xi_0^+) \\ \mathbf{X}^{(-)}(\xi_0^-) & \mathbf{0} \end{pmatrix} \mathbf{S},$$

where the unitary and symmetric scattering matrix $\mathbf{S}$

$$\mathbf{S} = \begin{pmatrix} \mathbf{R}_{\rightarrow} & \mathbf{T}_{\leftarrow} \\ \mathbf{T}_{\rightarrow} & \mathbf{R}_{\leftarrow} \end{pmatrix}, \quad \mathbf{S}^\dagger\mathbf{S} = \mathbf{S}\mathbf{S}^\dagger = \mathbf{I} \tag{11}$$

is composed of the matrices, whose elements are reflection and transmission amplitudes that enter Eqs. (9). These matrices possess the following properties (see [41] for details):

$$\mathbf{T}_{\rightarrow}^\dagger\mathbf{T}_{\rightarrow} + \mathbf{R}_{\rightarrow}^\dagger\mathbf{R}_{\rightarrow} = \mathbf{I}_{oo} = \mathbf{T}_{\leftarrow}^\dagger\mathbf{T}_{\leftarrow} + \mathbf{R}_{\leftarrow}^\dagger\mathbf{R}_{\leftarrow}, \tag{12}$$

$$\mathbf{T}_{\rightarrow}^\dagger\mathbf{R}_{\leftarrow} + \mathbf{R}_{\rightarrow}^\dagger\mathbf{T}_{\leftarrow} = \mathbf{0} = \mathbf{R}_{\leftarrow}^\dagger\mathbf{T}_{\rightarrow} + \mathbf{T}_{\leftarrow}^\dagger\mathbf{R}_{\rightarrow},$$

$$\mathbf{T}_{\rightarrow}^{\,T} = \mathbf{T}_{\leftarrow}, \quad \mathbf{R}_{\rightarrow}^{\,T} = \mathbf{R}_{\rightarrow}, \quad \mathbf{R}_{\leftarrow}^{\,T} = \mathbf{R}_{\leftarrow}.$$

If $V^{\text{pair}}(x_{ij}) = V^{\text{hosc}}(x_{ij})$, then the basis functions of $(A-1)$-dimensional oscillator $\Phi_j(\boldsymbol{\xi})$ corresponding to the energy $E_i = (2\sum_{k=1}^{A-1} i_k + A - 1)$ have the form:

$$\left(-\frac{\partial^2}{\partial\boldsymbol{\xi}^2} + \boldsymbol{\xi}^2 - E_j\right)\Phi_j(\boldsymbol{\xi}) = 0, \tag{13}$$

$$\int_{-\infty}^{+\infty} \Phi_i(\boldsymbol{\xi})\Phi_j(\boldsymbol{\xi})d^{A-1}\boldsymbol{\xi} = \delta_{ij}.$$

In the next section we describe the procedure of constructing the required sets of basis functions that depend on $A-1$ symmetrized internal coordinates and are symmetric (S) or antisymmetric (A) with respect to permutation of the initial A Cartezian coordinates of A identical particles and the corresponding eigenvalues for a cluster of A identical particles in the center-of-mass system (CMS), which we refer as *symmetrized coordinates representation*.

3. SYMMETRIZED COORDINATES REPRESENTATION

For simplicity, consider the solutions of Eq. (8) in the internal symmetrized coordinates $\{\xi_1, \ldots, \xi_{A-1}\} \in \mathbf{R}^{A-1}$, $x_i \in \mathbf{R}^1$, in the case of 1D Euclidean space ($d = 1$). The relevant equation describes an $(A-1)$-dimensional oscillator with the eigenfunctions $\Phi_j(\xi_1, \ldots, \xi_{A-1})$ and the energy eigenvalues E_j:

$$\left[\sum_{i=1}^{A-1}\left(-\frac{\partial^2}{\partial\xi_i^2} + (\xi_i)^2\right) - E_j\right] \times \Phi_j(\xi_1, \ldots, \xi_{A-1}) = 0,$$

$$E_j = 2\sum_{k=1}^{A-1} i_k + A - 1,$$

where the numbers i_k, $k = 1, \ldots, A-1$, are integer, $i_k = 0, 1, 2, 3, \ldots$ The eigenfunctions $\Phi_j(\xi_1, \ldots, \xi_{A-1})$ can be expressed in terms of the conventional eigenfunctions of individual 1D oscillators as

$$\Phi_j(\xi_1, \ldots, \xi_{A-1}) = \sum_{2\sum_{k=1}^{A-1} i_k + A - 1 = E_j} \beta_{j[i_1, i_2, \ldots, i_{A-1}]} \times \bar{\Phi}_{[i_1, i_2, \ldots, i_{A-1}]}(\xi_1, \ldots, \xi_{A-1}), \tag{15}$$

$$\bar{\Phi}_{[i_1, i_2, \ldots, i_{A-1}]}(\xi_1, \ldots, \xi_{A-1}) = \prod_{k=1}^{A-1} \bar{\Phi}_{i_k}(\xi_k),$$

$$\bar{\Phi}_{i_k}(\xi_k) = \frac{\exp(-\xi_k^2/2)H_{i_k}(\xi_k)}{\sqrt[4]{\pi}\sqrt{2^{i_k}}\sqrt{i_k!}},$$

where $H_{i_k}(\xi_k)$ are Hermite polynomials [42]. Generally, the energy level $E_f = 2f + A - 1$, $f = \sum_{k=1}^{A-1} i_k$, of an $(A-1)$-dimensional oscillator is known [43] to possess the degeneracy multiplicity $p = (A + f - 2)!/f!/(A-2)!$ with respect to the conventional oscillator eigenfunctions $\bar{\Phi}_{[i_1, i_2, \ldots, i_{A-1}]}(\xi_1, \ldots, \xi_{A-1})$. This degeneracy allows further symmetrization by choosing the appropriate coefficients $\beta^{(j)}_{[i_1, i_2, \ldots, i_{A-1}]}$. Degeneracy multiplicity p of all states with the given energy E_j is defined by formula

$$p = \sum_{2\sum_{k=1}^{A-1} i_k + A - 1 = E_j} N_\beta, \tag{16}$$

$$N_\beta = (A-1)! \Big/ \prod_{k=1}^{N_\upsilon} \upsilon_k!,$$

where N_β is the number of multiset permutations (m.p.) of $[i_1, i_2, \ldots, i_{A-1}]$, and $N_\upsilon \le A - 1$ is the number of different values i_k in the multiset $[i_1, i_2, \ldots, i_{A-1}]$, and υ_k is the number of repetitions of the given value i_k.

Step 1. Symmetrization with Respect to Permutation of $A-1$ Particles

For the states $\Phi_j^s(\xi_1, \ldots, \xi_{A-1}) \equiv \Phi^s_{[i_1, i_2, \ldots, i_{A-1}]} \times (\xi_1, \ldots, \xi_{A-1})$, symmetric with respect to permutation of $A-1$ particles $i = [i_1, i_2, \ldots, i_{A-1}]$, the coefficients $\beta_{i[i'_1, i'_2, \ldots, i'_{A-1}]}$ in Eq. (15) are

$$\beta_{i[i'_1, i'_2, \ldots, i'_{A-1}]} \tag{17}$$

Table 1. The eigenvalues $E^s_j = E^s_{[i_1,i_2,\ldots,i_{N-1}]}$ for the first oscillator symmetric eigenfunctions $\Phi^s_j(\xi_1,\ldots,\xi_{N-1}) = |[i_1,i_2,\ldots,i_{A-1}]\rangle = \Phi^s_{[i_1,i_2,\ldots,i_{A-1}]}(\xi_1,\ldots,\xi_{A-1})$ with $E^s_j - E^s_1 = 2\sum_{k=1}^{A-1} i_k \le 10$, $E^s_1 = A-1$ and corresponding number N_β of a multiset permutations $[i_1,i_2,\ldots,i_{A-1}]$ of quantum numbers $i_1,i_2,\ldots,i_{A-1}$ from (16) (see (17))

$A=3$			$A=4$			$A=5$			$A=6$			$E^s_j - E^s_1$
j	$\lvert[i_1,i_2]\rangle$	N_β	j	$\lvert[i_1,i_2,i_3]\rangle$	N_β	j	$\lvert[i_1,i_2,i_3,i_4]\rangle$	N_β	j	$\lvert[i_1,i_2,i_3,i_4,i_5]\rangle$	N_β	
1	$\lvert[0,0]\rangle$	1	1	$\lvert[0,0,0]\rangle$	1	1	$\lvert[0,0,0,0]\rangle$	1	1	$\lvert[0,0,0,0,0]\rangle$	1	0
2	$\lvert[0,1]\rangle$	2	2	$\lvert[0,0,1]\rangle$	3	2	$\lvert[0,0,0,1]\rangle$	4	2	$\lvert[0,0,0,0,1]\rangle$	5	2
3	$\lvert[0,2]\rangle$	2	3	$\lvert[0,0,2]\rangle$	3	3	$\lvert[0,0,0,2]\rangle$	4	3	$\lvert[0,0,0,0,2]\rangle$	5	
4	$\lvert[1,1]\rangle$	1	4	$\lvert[0,1,1]\rangle$	3	4	$\lvert[0,0,1,1]\rangle$	6	4	$\lvert[0,0,0,1,1]\rangle$	10	4
5	$\lvert[0,3]\rangle$	2	5	$\lvert[0,0,3]\rangle$	3	5	$\lvert[0,0,0,3]\rangle$	4	5	$\lvert[0,0,0,0,3]\rangle$	5	
6	$\lvert[1,2]\rangle$	2	6	$\lvert[0,1,2]\rangle$	6	6	$\lvert[0,0,1,2]\rangle$	12	6	$\lvert[0,0,0,1,2]\rangle$	20	6
			7	$\lvert[1,1,1]\rangle$	1	7	$\lvert[0,1,1,1]\rangle$	4	7	$\lvert[0,0,1,1,1]\rangle$	10	
7	$\lvert[0,4]\rangle$	2	8	$\lvert[0,0,4]\rangle$	3	8	$\lvert[0,0,0,4]\rangle$	4	8	$\lvert[0,0,0,0,4]\rangle$	5	
8	$\lvert[1,3]\rangle$	2	9	$\lvert[0,1,3]\rangle$	6	9	$\lvert[0,0,1,3]\rangle$	12	9	$\lvert[0,0,0,1,3]\rangle$	20	
9	$\lvert[2,2]\rangle$	1	10	$\lvert[0,2,2]\rangle$	3	10	$\lvert[0,0,2,2]\rangle$	6	10	$\lvert[0,0,0,2,2]\rangle$	10	8
			11	$\lvert[1,1,2]\rangle$	3	11	$\lvert[0,1,1,2]\rangle$	12	11	$\lvert[0,0,1,1,2]\rangle$	30	
						12	$\lvert[1,1,1,1]\rangle$	1	12	$\lvert[0,1,1,1,1]\rangle$	5	
10	$\lvert[0,5]\rangle$	2	12	$\lvert[0,0,5]\rangle$	3	13	$\lvert[0,0,0,5]\rangle$	4	13	$\lvert[0,0,0,0,5]\rangle$	5	
11	$\lvert[1,4]\rangle$	2	13	$\lvert[0,1,4]\rangle$	6	14	$\lvert[0,0,1,4]\rangle$	12	14	$\lvert[0,0,0,1,4]\rangle$	20	
12	$\lvert[2,3]\rangle$	2	14	$\lvert[0,2,3]\rangle$	6	15	$\lvert[0,0,2,3]\rangle$	12	15	$\lvert[0,0,0,2,3]\rangle$	20	
			15	$\lvert[1,1,3]\rangle$	3	16	$\lvert[0,1,1,3]\rangle$	12	16	$\lvert[0,0,1,1,3]\rangle$	30	10
			16	$\lvert[1,2,2]\rangle$	3	17	$\lvert[0,1,2,2]\rangle$	12	17	$\lvert[0,0,1,2,2]\rangle$	30	
						18	$\lvert[1,1,1,2]\rangle$	4	18	$\lvert[0,1,1,1,2]\rangle$	20	
									19	$\lvert[1,1,1,1,1]\rangle$	1	

$$= \begin{cases} \frac{1}{\sqrt{N_\beta}}, & \text{if } [i'_1,i'_2,\ldots,i'_{A-1}] \text{ is a multiset} \\ \text{permutation of } [i_1,i_2,\ldots,i_{A-1}]; \\ 0, \quad \text{otherwise.} \end{cases}$$

In Table 1 we demonstrate the rules of correspondence between the multisets of quantum numbers $[i_1,i_2,\ldots,i_{A-1}]$ and the numbers j of the eigenfunctions $\Phi^s_j(\xi_1,\ldots,\xi_{A-1})$ for symmetric states of an $(A-1)$-dimensional harmonic oscillator with the energy eigenvalues E^s_j, enumerated in nondecreasing order, $E^s_1 = A-1 < E^s_2 \le E^s_3 \le E^s_4 \le \ldots$, for A particles with the degenerate spectrum $E^s_j = 2\sum_{k=1}^{A-1} i_k + A - 1$. The corresponding isolines of the first eight symmetric oscillator eigenfunctions $\Phi^s_{[i_1,i_2]}(\xi_1,\xi_2)$ for $A=3$ are shown in Fig. 3.

With increasing A for given $E' = E^s_j - E^s_1$ the multiplicity of degeneracy, i.e., the number $p_s \le p$ of symmetric eigenfunctions, corresponding to the same eigenvalue, sharply increases and reaches a plateau. At fixed A with increasing E' the multiplicity increases faster, when A is larger. For example, the eigenvalue $E'=6$ at $A=2$ is nondegenerate ($p_s = 1$), at $A=3$ it is doubly degenerate ($p_s=2$), and at large $A \ge 4$ it is triply degenerate ($p_s=3$). For $A=4$, when the eigenvalue increases from $E'=8$ to $E'=10$, the multiplicity increases from $p_s=4$ to $p_s=5$, while for $A=6$ under the same conditions the multiplicity increases from $p_s=5$ to $p_s=7$.

For example, we can construct the states, antisymmetric with respect to permutation of $A-1$ particles with spin $1/2$, in a conventional way as a product of two determinants of $K \times K$ and $[(A-1)K] \times [(A-1)K]$ matrices, involving K and $[(A-1)K]$ states of pairs of particles with compensated and noncompensated spins, respectively, such that the total spin equals $(A-1)/2 - K$ [22, 23]. For

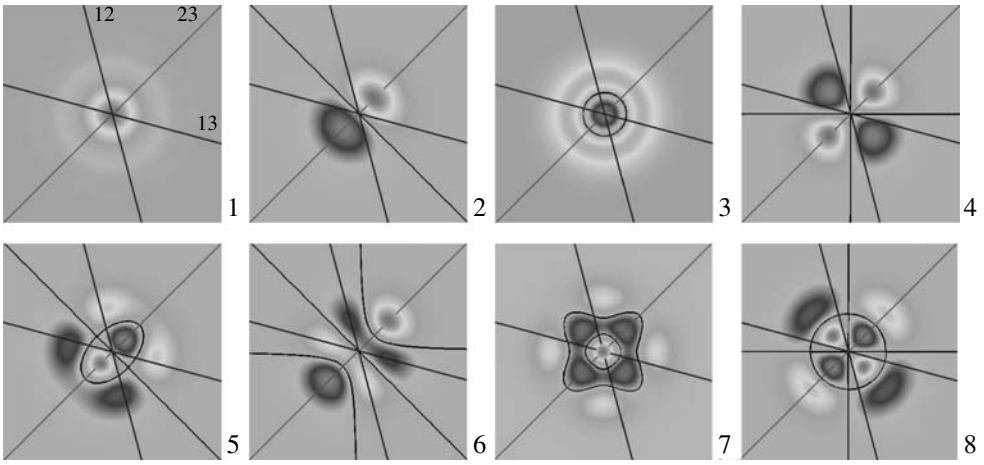

Fig. 3. Profiles of the first eight oscillator s eigenfunctions $\Phi^s_{[i_1,i_2]}(\xi_1,\xi_2)$, at $A=3$ in the coordinate frame (ξ_1,ξ_2). The lines correspond to pair collision $x_2=x_3$, $x_1=x_2$ and $x_1=x_3$ of projection $(x_1,x_2,x_3)\to(\xi_1,\xi_2)$ marked only in the left upper panel by 23, 12, and 13, respectively. The additional lines are nodes of the eigenfunctions $\Phi^s_{[i_1,i_2]}(\xi_1,\xi_2)$.

simplicity we consider a restricted case. The states $\Phi^a_j(\xi_1,\ldots,\xi_{A-1})\equiv\Phi^a_{[i_1,i_2,\ldots,i_{A-1}]}(\xi_1,\ldots,\xi_{A-1})$, antisymmetric with respect to permutation of $A-1$ particles, are constructed in a conventional way

$$\Phi^a_{[i_1,i_2,\ldots,i_{A-1}]}(\xi_1,\ldots,\xi_{A-1})=\frac{1}{\sqrt{(A-1)!}} \quad (18)$$
$$\times\begin{vmatrix} \bar\Phi_{i_1}(\xi_1) & \bar\Phi_{i_2}(\xi_1) & \cdots & \bar\Phi_{i_{A-1}}(\xi_1)\\ \bar\Phi_{i_1}(\xi_2) & \bar\Phi_{i_2}(\xi_2) & \cdots & \bar\Phi_{i_{A-1}}(\xi_2)\\ \vdots & \vdots & \ddots & \vdots\\ \bar\Phi_{i_1}(\xi_{A-1}) & \bar\Phi_{i_2}(\xi_{A-1}) & \cdots & \bar\Phi_{i_{A-1}}(\xi_{A-1})\end{vmatrix},$$

i.e., the coefficients $\beta_{i[i'_1,i'_2,\ldots,i'_{A-1}]}$ in Eq. (15) are expressed as $\beta_{i[i'_1,i'_2,\ldots,i'_{A-1}]}=\varepsilon_{i'_1,i'_2,\ldots,i'_{A-1}}/\sqrt{(A-1)!}$, where $\varepsilon_{i'_1,i'_2,\ldots,i'_{A-1}}$ is a totally antisymmetric tensor. This tensor is defined as follows: $\varepsilon_{i'_1,i'_2,\ldots,i'_{A-1}}=+1(-1)$ if $i'_1,i'_2,\ldots,i'_{A-1}$ is an even (odd) permutation of the numbers $i_1<i_2<\ldots<i_{A-1}$ and $\varepsilon_{i'_1,i'_2,\ldots,i'_{A-1}}=0$ otherwise, i.e., when some two numbers in the set $i'_1,i'_2,\ldots,i'_{A-1}$ are equal. Therefore, for antisymmetric states the indices i_k in Eq. (14) take the integer values $i_k=k-1,k,k+1,\ldots;\ k=1,\ldots,A-1$.

Table 2 demonstrates the rules of correspondence between the multisets of quantum numbers $[i_1,i_2,\ldots,i_{A-1}]$ and the numbers j of the eigenfunctions $\Phi^a_j(\xi_1,\ldots,\xi_{A-1})$ for antisymmetric states of an $(A-1)$-dimensional harmonic oscillator with the energy eigenvalues E^a_j, enumerated in nondecreasing order, $E^a_1=(A-1)^2<E^a_2\le E^a_3\le E^a_4\le\ldots$, for A particles with the degenerate spectrum $E^a_j=2\sum_{k=1}^{A-1}i_k+A-1$. For given $E'=E^a_j-E^a_1$ the number $p_a<p$ of degenerate antisymmetric eigenfunctions is seen to equal the number $p_s^{A-1}\le p$ of symmetric eigenfunctions with the same $E'=E^s_j-E^s_1$. Note, that the multisets, characterizing symmetric states, are related with the sets, characterizing antisymmetric states, by the following rule: the first number is left unchanged, from the second number we subtract one, from the third one we subtract two, and so on. The corresponding isolines of the first eight oscillator antisymmetric eigenfunctions $\Phi^a_{[i_1,i_2]}(\xi_1,\xi_2)$ for $A=3$ are shown in Fig. 4.

Here and below the indexes s and a are used for the functions, symmetric (antisymmetric) under permutations of $A-1$ relative coordinates, constructed at the first step of the procedure. On the contrary, indexes S and A are used for functions, symmetric (asymmetric) under permutations of A initial Cartesian coordinates. This is actually a symmetry with respect to permutation of identical particles themselves; in this sense S and A states may be attributed to boson- and fermion-like particles. However, we prefer to use the S (A) notation as more rigorous.

Step 2. Symmetrization with Respect to Permutation of A Particles

For $A=2$ the symmetrized coordinate ξ_1 corresponds to the difference x_2-x_1 of Cartesian coordinates, so that a function even (odd) with respect to ξ_1 appears to be symmetric (antisymmetric) with respect to the permutation of two particles $x_2\leftrightarrow x_1$. Hence, even (odd) eigenfunctions with corresponding eigenvalues $E^s_j=2(2n)+1$ ($E^a_j=2(2n+1)+1$) describe S (A) solutions.

Table 2. The eigenvalues $E^a_j = E^a_{[i_1,i_2,\ldots,i_{A-1}]}$ for the first oscillator antisymmetric eigenfunctions $\Phi^a_j(\xi_1,\ldots,\xi_{A-1}) = |[i_1,i_2,\ldots,i_{A-1}]\rangle = \Phi^a_{[i_1,i_2,\ldots,i_{A-1}]}(\xi_1,\ldots,\xi_{A-1})$ from (18) with $E^a_j - E^a_1 \le 10$, $E^a_1 = (A-1)^2$

$A=3$, $E^a_1=4$		$A=4$, $E^a_1=9$		$A=5$, $E^a_1=16$		$E^a_j - E^a_1$
j	$\lvert[i_1,i_2]\rangle$	j	$\lvert[i_1,i_2,i_3]\rangle$	j	$\lvert[i_1,i_2,i_3,i_4]\rangle$	
1	$\lvert[0,1]\rangle$	1	$\lvert[0,1,2]\rangle$	1	$\lvert[0,1,2,3]\rangle$	0
2	$\lvert[0,2]\rangle$	2	$\lvert[0,1,3]\rangle$	2	$\lvert[0,1,2,4]\rangle$	2
3	$\lvert[1,2]\rangle$	3	$\lvert[0,2,3]\rangle$	3	$\lvert[0,1,3,4]\rangle$	
4	$\lvert[0,3]\rangle$	4	$\lvert[0,1,4]\rangle$	4	$\lvert[0,1,2,5]\rangle$	4
5	$\lvert[1,3]\rangle$	5	$\lvert[1,2,3]\rangle$	5	$\lvert[0,2,3,4]\rangle$	
6	$\lvert[0,4]\rangle$	6	$\lvert[0,2,4]\rangle$	6	$\lvert[0,1,3,5]\rangle$	6
		7	$\lvert[0,1,5]\rangle$	7	$\lvert[0,1,2,6]\rangle$	
7	$\lvert[2,3]\rangle$	8	$\lvert[1,2,4]\rangle$	8	$\lvert[1,2,3,4]\rangle$	
8	$\lvert[1,4]\rangle$	9	$\lvert[0,3,4]\rangle$	9	$\lvert[0,2,3,5]\rangle$	
9	$\lvert[0,5]\rangle$	10	$\lvert[0,2,5]\rangle$	10	$\lvert[0,1,4,5]\rangle$	8
		11	$\lvert[0,1,6]\rangle$	11	$\lvert[0,1,3,6]\rangle$	
				12	$\lvert[0,1,2,7]\rangle$	
10	$\lvert[2,4]\rangle$	12	$\lvert[1,3,4]\rangle$	13	$\lvert[1,2,3,5]\rangle$	
11	$\lvert[1,5]\rangle$	13	$\lvert[1,2,5]\rangle$	14	$\lvert[0,2,4,5]\rangle$	
12	$\lvert[0,6]\rangle$	14	$\lvert[0,3,5]\rangle$	15	$\lvert[0,2,3,6]\rangle$	10
		15	$\lvert[0,2,6]\rangle$	16	$\lvert[0,1,4,6]\rangle$	
		16	$\lvert[0,1,7]\rangle$	17	$\lvert[0,1,3,7]\rangle$	
				18	$\lvert[0,1,2,8]\rangle$	

For $A \ge 3$ the functions symmetric (antisymmetric) with respect to permutations of Cartesian coordinates $x_{i+1} \leftrightarrow x_{j+1}$, $i,j = 0,\ldots,A-1$: $\Phi^{S(A)}(\ldots,x_{i+1},\ldots,x_{j+1},\ldots) \equiv \Phi^{S(A)}(\xi_1(x_1,\ldots,x_A),\ldots,\xi_{A-1}(x_1,\ldots,x_A)) = \pm\Phi^{S(A)}(\ldots,x_{j+1},\ldots,x_{i+1},\ldots)$ become symmetric (antisymmetric) with respect to permutations of symmetrized coordinates $\xi_i \leftrightarrow \xi_j$, $i,j = 1,\ldots,A-1$: $\Phi^{S(A)}(\ldots,\xi_i,\ldots,\xi_j,\ldots) = \pm\Phi^{S(A)}(\ldots,\xi_j,\ldots,\xi_i,\ldots)$, as follows from Eq. (5). However, the converse statement is not valid, $\Phi^{s(a)}(\ldots,\xi_i,\ldots,\xi_j,\ldots) = \pm\Phi^{s(a)}(\ldots,\xi_j,\ldots,\xi_i,\ldots) \not\Rightarrow \Phi^{s(a)}(x_1,\ldots,x_{i+1},\ldots) = \pm\Phi^{s(a)}(x_{i+1},\ldots,x_1,\ldots)$, because we deal with a projection map $(\xi_1,\ldots,\xi_{A-1})^T = \hat{C}(x_1,\ldots,x_A)^T$, which is implemented by the $(A-1)\times A$ matrix $\hat{C}$ with the matrix elements $\hat{C}_{ij} = C_{i+1,j}$, obtained from (4) by cancelling the first row. Hence, the functions, symmetric (antisymmetric) with respect to permutations of symmetrized coordinates, are divided into two types, namely, the S (A) solutions, symmetric (antisymmetric) with respect to permutations $x_1 \leftrightarrow x_{j+1}$ at $j = 1,\ldots,A-1$:

$$\Phi^{S(A)}(x_1,\ldots,x_{i+1},\ldots)$$
$$\equiv \Phi^{S(A)}(\xi_1(x_1,\ldots,x_A),\ldots,\xi_{A-1}(x_1,\ldots,x_A))$$
$$= \pm\Phi^{S(A)}(x_{i+1},\ldots,x_1,\ldots),$$

and the other s (a) solutions, $\Phi^{s(a)}(x_1,\ldots,x_{i+1},\ldots) \ne \pm\Phi^{s(a)}(x_{i+1},\ldots,x_1,\ldots)$, which should be eliminated. These requirements are equivalent to only one permutation $x_1 \leftrightarrow x_2$, as follows from (5), which simplifies their practical implementation. With these requirements taken into account in the Gram–Schmidt process, implemented in a *symbolic algorithm SCR*, we obtained the required characteristics of S and A eigenfunctions

$$\Phi^{S(A)}_i(\xi_1,\ldots,\xi_{A-1}) \qquad (19)$$

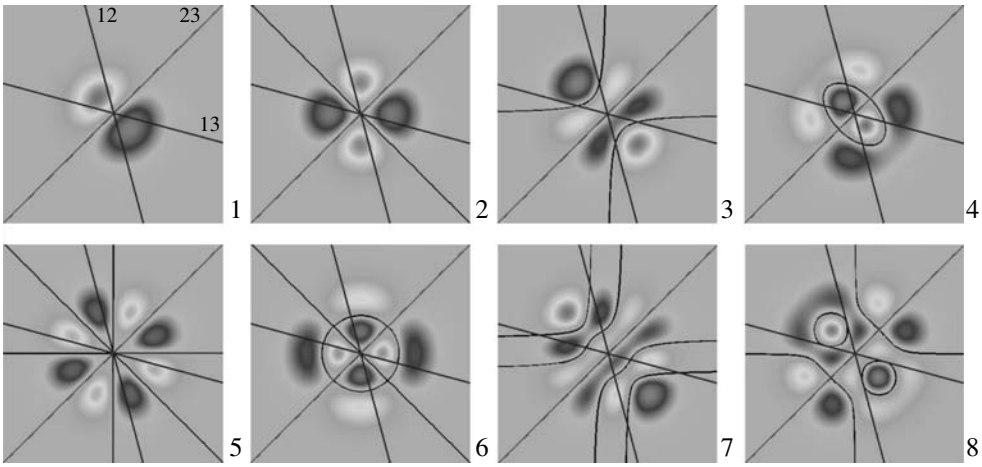

Fig. 4. The same as in Fig. 3, but for the first eight oscillator a eigenfunctions $\Phi^{a}_{[i_1,i_2]}(\xi_1,\xi_2)$, at $A=3$.

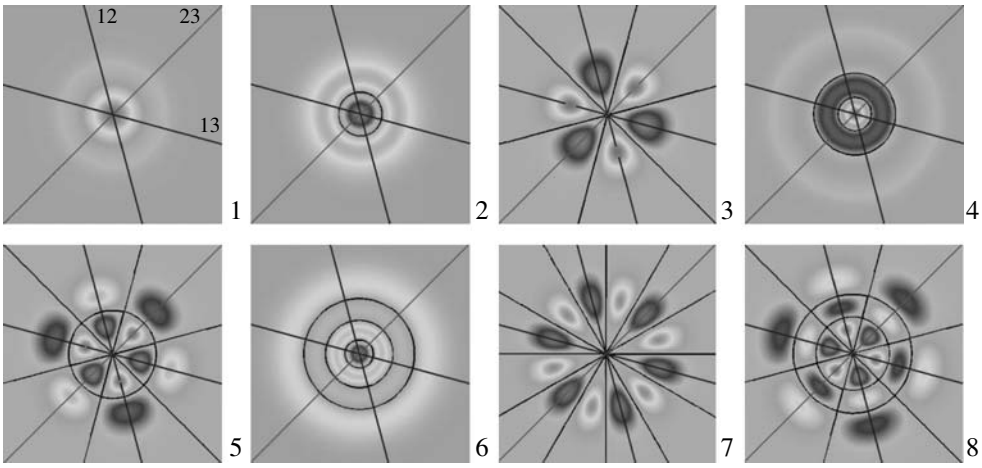

Fig. 5. The same as in Fig. 3, but for the first eight oscillator S eigenfunctions $\Phi^{S}_{[i_1,i_2]}(\xi_1,\xi_2)$, at $A=3$.

$$= \sum_{2\sum_{k=1}^{A-1} i_k + A - 1 = E_i^{s(a)}} \alpha^{S(A)}_{i[i_1,i_2,\ldots,i_{A-1}]} \times \Phi^{s(a)}_{[i_1,i_2,\ldots,i_{A-1}]}(\xi_1,\ldots,\xi_{A-1})$$

with respect to permutations of A identical particles, the examples of which are presented in Tables 3 and 4. Note, that for $A=4$ the first four states from Table 3 are similar to those of the translation-invariant model without excitation of the center-of-mass variable [37]. This SCR algorithm was implemented in Maple and published in [44].

As an example, in Figs. 5 and 6 we show isolines of the first eight S and A oscillator eigenfunctions $\Phi^{S}_{[i_1,i_2]}(\xi_1,\xi_2)$ and $\Phi^{A}_{[i_1,i_2]}(\xi_1,\xi_2)$ for $A=3$, calculated at the second step of the algorithm. One can see that the S (A) oscillator eigenfunctions are symmetric (antisymmetric) with respect to reflections from three straight lines. The first line (labelled 23) corresponds to the permutation $(x_2,\ x_3)$ and is rotated by $\pi/4$ counterclockwise with respect to the axis ξ_1. The second and the third lines (labelled 12 and 13) correspond to the permutations $(x_1,\ x_2)$ and $(x_1,\ x_3)$ and are rotated by $\pi/3$ clockwise and counterclockwise with respect to the first line. These lines divide the plane into six sectors, while the symmetric (antisymmetric) oscillator eigenfunctions, calculated at the first step of the algorithm, which are symmetric (or antisymmetric) with respect to reflections from the first line, generate the division of the plane into two parts.

The Jacobi coordinates $(y_1,\ y_2)$ are related to the symmetrized coordinates $(\xi_1,\ \xi_2)$ via the orthogonal transformation (6), i.e., the permutation of coordinates $(\xi_1,\xi_2) \to (\xi_2,\xi_1)$ and the clockwise rotation by the angle $\phi_1 = \pi/12$. Therefore, in the Jacobi coordinates the lines, corresponding to pair collisions of the particles $(x_2,\ x_3)$, $(x_1,\ x_2)$, and $(x_1,\ x_3)$, will be also clockwise rotated by the angle $\phi_1 = \pi/12$.

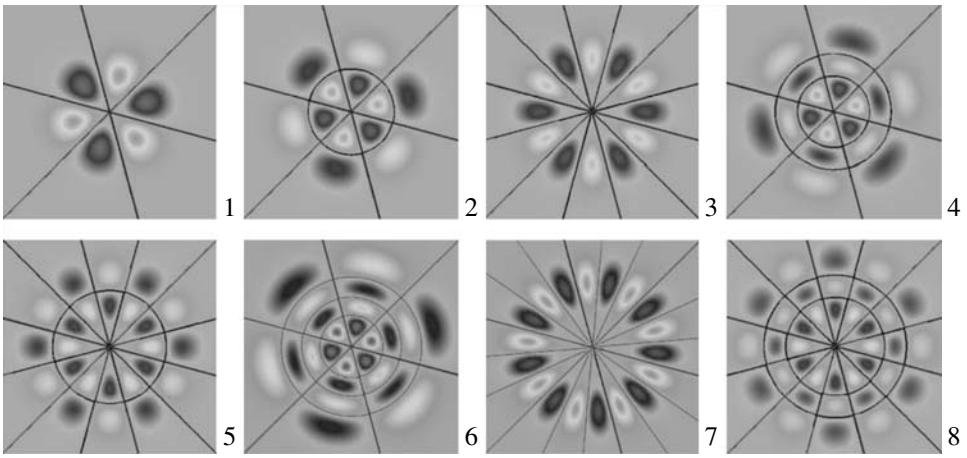

Fig. 6. The same as in Fig. 3, but for the first eight oscillator A eigenfunctions $\Phi^{A}_{[i_1,i_2]}(\xi_1,\xi_2)$, at $A=3$.

Counterclockwise rotation of the coordinate system $(\xi_2,\ \xi_1)$ to $(y_1,\ y_2)$ by the angle $\phi_1=\pi/12$ induces a unitary transformation of the corresponding $(A=2)$-oscillator functions $\langle\xi_2,\xi_1|i_2,i_1\rangle=\bar{\Phi}_{[i_2,i_1]}(\xi_2,\xi_1)$ with $j=(i_2+i_1)/2$:

$$\langle j+m',j-m'|y_1,y_2\rangle$$
$$=\sum_{m=-j}^{m=j}\langle j+m',j-m'|G_{21}(\phi_1)|j+m,j-m\rangle$$
$$\times\langle j+m,j-m|\xi_2,\xi_1\rangle.$$

The matrix elements $\langle j+m',j-m'|G_{21}(\phi_1)|j+m,j-m\rangle$ are expressed as the integrals [45]:

$$\langle j+m',j-m'|G_{21}(\phi)|j+m,j-m\rangle$$
$$=d^{j}_{m'm}(2\phi_1)=\int\limits_{-\infty}^{\infty}\int\limits_{-\infty}^{\infty}d\xi_2d\xi_1\langle j+m',$$
$$j-m'|\xi_2\cos\phi_1+\xi_1\sin\phi_1,$$
$$-\xi_2\sin\phi_1+\xi_1\cos\phi_1\rangle$$
$$\times\langle\xi_2,\xi_1|j+m,j-m\rangle,$$

where

$$d^{j}_{m'm}(2\phi_1)=N^{j}_{m'm}\sin^{|m'-m|}\phi_1$$
$$\times\cos^{|m'+m|}\phi_1P^{|m'-m|,|m'+m|}_{j-(|m'-m|+|m'+m|)/2}(\cos(2\phi_1))$$

are Wigner functions [46], $N^{j}_{m'm}$ are the normalization factors, $P^{\mu\nu}_{s}(x)$ are Jacobi polynomials [42]. This is the simplest integral representation of *the oscillator Wigner functions* [47].

Figure 7 shows examples of profiles of S and A oscillator eigenfunctions $\Phi^{S,A}_{[i_1,i_2,i_3]}(\xi_1,\xi_2,\xi_3)$ for $A=4$. Note that four maxima (black) and four minima (grey) of the S eigenfunction $\Phi^{S}_{[1,1,1]}(\xi_1,\xi_2,\xi_3)$ are positioned at the vertices of two tetrahedrons forming a *stella octangula*, with the edges shown by black and grey lines, respectively. Eight maxima and six outer minima for S eigenfunction $\Phi^{S}_{[0,0,4]}(\xi_1,\xi_2,\xi_3)$ are positioned at the vertices of a cube and an octahedron, the edges of which are shown by black and grey lines, respectively. The positions of twelve maxima of the A oscillator eigenfunction, $\Phi^{A}_{[0,2,4]}(\xi_1,\xi_2,\xi_3)$ coincide with the vertices of a polyhedron with 20 triangle faces (only 8 of them being equilateral triangles) and 30 edges, 6 of them having the length 2.25 and the other having the length 2.66.

For $A=4$ the 3D rotation (7), reducing the coordinate system (ξ_1,ξ_2,ξ_3) to $(y_1,y_2,y_3,)$, can be presented as a product of three counterclockwise rotations $M=M_3(\phi_3)M_2(\phi_2)M_1(\phi_1)$ in separate coordinate planes: by the angle $\phi_1=3\pi/4$ about the first old axis, ξ_1, by the angle $\phi_2=\pi-\arctan(\sqrt{2})\approx 16\pi/23$ about the third new axis, ξ_3', and by the angle $\phi_3=\pi/3$ about the first new axis, $y_1=\xi_1''$ (see Fig. 2). This 3D rotation induces a unitary transformation of the corresponding $(A=3)$-oscillator functions $\langle\xi_1,\xi_2,\xi_3|i_1,i_2,i_3\rangle=\bar{\Phi}_{[i_1,i_2,i_3]}(\xi_1,\xi_2,\xi_3)$, $n=i_1+i_2+i_3$:

$$\langle j'+m',j'-m',n-2j'|y_1,y_2,y_3\rangle$$
$$=\sum_{j=0}^{n/2}\sum_{m=-j}^{m=j}\langle j'+m',j'-m',$$
$$n-2j'|G(3)|j+m,j-m,n-2j\rangle$$
$$\times\langle j+m,j-m,n-2j|\xi_1,\xi_2,\xi_3\rangle.$$

Here the matrix elements $\langle j'+m',j-m',$ $n-2j'|G(3)|j+m,j-m,n-2j\rangle$ are defined as [45]

$$\langle j'+m',j'-m',$$

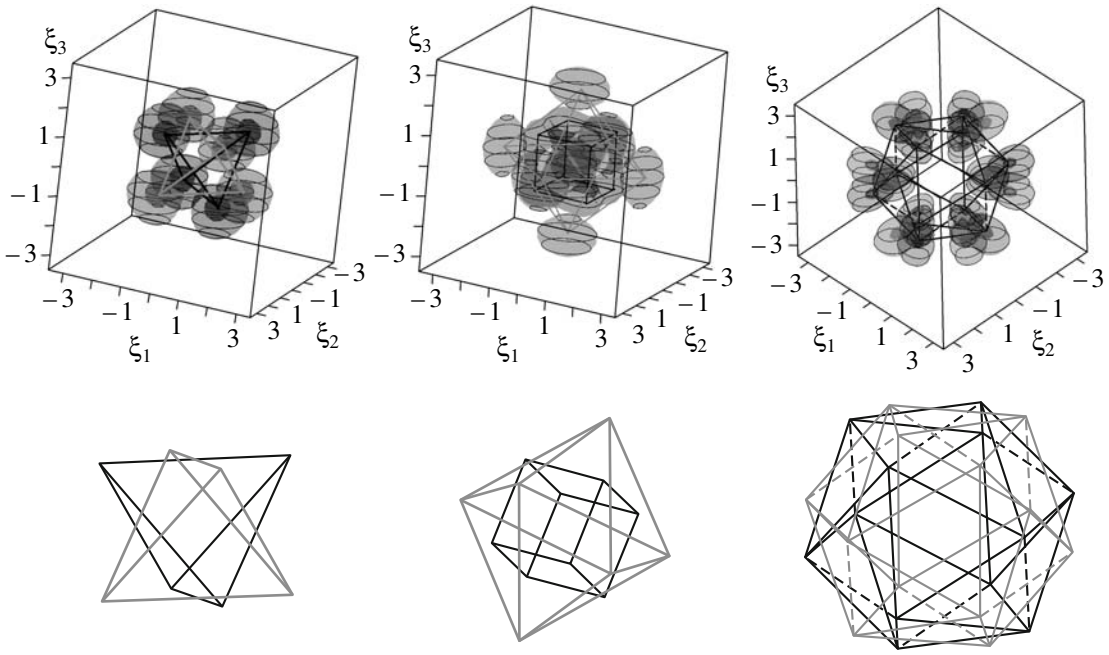

Fig. 7. (Upper panels) Profiles of the oscillator S eigenfunctions $\Phi^S_{[1,1,1]}(\xi_1,\xi_2,\xi_3)$, $\Phi^S_{[0,0,4]}(\xi_1,\xi_2,\xi_3)$ and A eigenfunction $\Phi^A_{[0,2,4]}(\xi_1,\xi_2,\xi_3)$, at $A=4$ (left, middle, and right panels, respectively). (Lower panels) Some maxima and minima positions of these functions are connected by black and gray lines and duplicated: two tetrahedrons forming a *stella octangula* for $\Phi^S_{[1,1,1]}(\xi_1,\xi_2,\xi_3)$, a cube and an octahedron for $\Phi^S_{[0,0,4]}(\xi_1,\xi_2,\xi_3)$, and a polyhedron with 20 triangle faces (only 8 of them being equilateral triangles) and 30 edges, 6 of them having the length 2.25 and the other having the length 2.66 for $\Phi^A_{[0,2,4]}(\xi_1,\xi_2,\xi_3)$.

$$n-2j'|G_{2,3}(\phi_3)G_{1,2}(\phi_2)G_{2,3}(\phi_1)|j+m,$$
$$j-m,n-2j\rangle$$
$$=\sum_t^{\min(j,j')} d^{j'}_{t-j',m'}(2\phi_3)d^{(n-t)/2}_{2j'-(n+t)/2,2j-(n+t)/2}$$
$$\times(2\phi_2)d^{j}_{m,t-j}(2\phi_1),$$

where the values of t are such that the absolute values of all t-dependent subscripts in the Wigner d functions do not exceed those of the superscripts.

In the general case, the transformations of $(A-1)$-dimensional oscillator functions induced by permutation of coordinates and $(A-1)$-dimensional finite rotation, presented as a product of $(A-1)(A-2)/2$ rotations in separate coordinate planes, can be constructed using the diagram method, which reduces the analytic calculations of the $(A-1)$-dimensional *oscillator Wigner functions* to simple geometric operations [47].

The degeneracy multiplicity (16), i.e., the number p of all states with the given energy E_j, the numbers p_s (p_a) of the states, symmetric (antisymmetric) under permutations of $A-1$ relative coordinates together with the total numbers p_S (p_A) of the states, symmetric (antisymmetric) under permutations of A initial Cartesian coordinates are summarized in Table 5 for the bottom part of the energy spectrum.

Note that the S and A states with $E'=E_1^{S,A}+2$ do not exist. The numbers p_s (p_a) are essentially smaller than the total number p of all states, which simplifies the procedure of constructing S (A) states with possible excitation of the center-of-mass degree of freedom and allows the use of a compact basis with the reduced degeneracy p_S (p_A) of the S (A) states in our final calculations. For clarity, in the case $A=3$, $d=1$, the S (A)-type functions generated by the SCR algorithm, in polar coordinates $\xi_1=\rho\cos\varphi$, $\xi_2=\rho\sin\varphi$ are expressed as:

$$\Phi^{S(A)}_{k,m}(\rho,\varphi)=C_{km}(\rho^2)^{3m/2} \qquad (20)$$
$$\times\exp(-\rho^2/2)L^{3m}_k(\rho^2)\begin{matrix}\cos\\ \sin\end{matrix}(3m(\varphi+\pi/12)),$$

where C_{km} is the normalization constant, $L^{3m}_k(\rho^2)$ are the Laguerre polynomials [42], $k=0,1,\ldots$, $m=0,1,\ldots$ for S states, while $m=1,2,\ldots$ for A states, that are classified by irreducible representations of the D_{3m} symmetry group. The corresponding energy levels $E^{S(A)}_{k,m}=2(2k+3m+1)=E^{s(a)}_{[i_1,i_2]}=2(i_1+i_2+1)$ have the degeneracy multiplicity $K+1$, if the energy $E^{S(A)}_{k,m}-E^{S(A)}_1=12K+K'$, where $K'=$

Table 3. The first few eigenvalues E_j^S and the oscillator S eigenfunctions (19) at $E_j^S - E_1^S \le 10$, $E_1^S = A-1$ (We use the notations $|[i_1,i_2,\ldots,i_{A-1}]\rangle \equiv \Phi^s_{[i_1,i_2,\ldots,i_{A-1}]}(\xi_1,\ldots,\xi_{A-1})$ from Eqs. (15) and (17), i.e. $[i_1,i_2,\ldots,i_{A-1}]$ assumes the summation over permutations of $[i_1,i_2,\ldots,i_{A-1}]$ in the layer $2\sum_{k=1}^{A-1} i_k + A - 1 = E_i^{s(a)}$)

$A=2$		$A=3$		$A=4$		$A=5$		$E_j^S - E_1^S$
j	$\Phi_j^S(\xi_1)$	j	$\Phi_j^S(\xi_1,\xi_2)$	j	$\Phi_j^S(\xi_1,\xi_2,\xi_3)$	j	$\Phi_j^S(\xi_1,\xi_2,\xi_3,\xi_4)$	
1	$\|[0]\rangle$	1	$\|[0,0]\rangle$	1	$\|[0,0,0]\rangle$	1	$\|[0,0,0,0]\rangle$	0
2	$\|[2]\rangle$	2	$\|[0,2]\rangle$	2	$\|[0,0,2]\rangle$	2	$\|[0,0,0,2]\rangle$	4
		3	$\frac{1}{2}\|[0,3]\rangle - \frac{\sqrt{3}}{2}\|[1,2]\rangle$	3	$\|[1,1,1]\rangle$	3	$\approx -0.27\|[0,0,0,3]\rangle + 0.27\|[0,0,1,2]\rangle$	6
							$-0.93\|[0,1,1,1]\rangle$	
3	$\|[4]\rangle$	4	$\frac{\sqrt{3}}{2}\|[0,4]\rangle + \frac{1}{2}\|[2,2]\rangle$	4	$\|[0,0,4]\rangle$	4	$\frac{\sqrt{2}}{2}\|[0,0,0,4]\rangle + \frac{\sqrt{2}}{2}\|[0,0,2,2]\rangle$	
				5	$\|[0,2,2]\rangle$	5	$\approx -0.32\|[0,0,0,4]\rangle - 0.39\|[0,0,1,3]\rangle$	8
							$+ 0.32\|[0,0,2,2]\rangle + 0.67\|[0,1,1,2]\rangle$	
							$- 0.44\|[1,1,1,1]\rangle$	
		5	$\frac{\sqrt{5}}{4}\|[0,5]\rangle - \frac{3}{4}\|[1,4]\rangle$	6	$\|[1,1,3]\rangle$	6, 7	Two functions	10
			$-\frac{\sqrt{2}}{4}\|[2,3]\rangle$					

Table 4. The first few eigenvalues E_j^A and the oscillator A eigenfunctions (19) at $E_j^A - E_1^A \le 10$, $E_1^A = A^2 - 1$ (We use the notations $|[i_1,i_2,\ldots,i_{A-1}]\rangle \equiv \Phi^a_{[i_1,i_2,\ldots,i_{A-1}]}(\xi_1,\ldots,\xi_{A-1})$ from Eq. (18), i.e. $[i_1,i_2,\ldots,i_{A-1}]$ assumes the summation over the multiset permutations of $[i_1,i_2,\ldots,i_{A-1}]$ in the layer $2\sum_{k=1}^{A-1} i_k + A - 1 = E_i^{s(a)}$)

$A=2$, $E_1^A=3$		$A=3$, $E_1^A=8$		$A=4$, $E_1^A=15$		$E_j^A - E_1^A$
j	$\Phi_j^A(\xi_1)$	j	$\Phi_j^A(\xi_1,\xi_2)$	j	$\Phi_j^A(\xi_1,\xi_2,\xi_3)$	
1	$\|[1]\rangle$	1	$\frac{1}{2}\|[0,3]\rangle + \frac{\sqrt{3}}{2}\|[1,2]\rangle$	1	$\|[0,2,4]\rangle$	0
2	$\|[3]\rangle$	2	$\frac{\sqrt{5}}{4}\|[0,5]\rangle + \frac{3}{4}\|[1,4]\rangle - \frac{\sqrt{2}}{4}\|[2,3]\rangle$	2	$\|[0,2,6]\rangle$	4
		3	$\frac{1}{4}\|[0,6]\rangle - \frac{\sqrt{15}}{4}\|[2,4]\rangle$	3	$\|[1,3,5]\rangle$	6
3	$\|[5]\rangle$	4	$\frac{\sqrt{21}}{8}\|[0,7]\rangle + \frac{3\sqrt{3}}{8}\|[1,6]\rangle - \frac{1}{8}\|[2,5]\rangle + \frac{\sqrt{5}}{8}\|[3,4]\rangle$	4	$\|[0,4,6]\rangle$	
				5	$\|[0,2,8]\rangle$	8
		5	$\frac{\sqrt{2}}{4}\|[0,8]\rangle - \frac{\sqrt{14}}{4}\|[2,6]\rangle$	6	$\|[1,3,7]\rangle$	10

$0,4,6,8,10,14$. For example, in Figs. 5 and 6 we show the wave functions $\Phi^S_{3,0}(\rho,\varphi)$ and $\Phi^S_{0,2}(\rho,\varphi)$ (or $\Phi^A_{3,1}(\rho,\varphi)$ and $\Phi^A_{0,3}(\rho,\varphi)$) labelled with 6 and 7, corresponding to the energy levels $E^{S(A)}_{k,m} - E^{S(A)}_1 = 12$ with the degeneracy $K=2$, while the functions labelled with $1,2,3,4,5,8$ are nondegenerate ($K=1$). From our calculation we conclude that the eigenfunctions of the A identical particle system in one dimension are degenerate like in [48], and this result disagrees with [49]. The latter can be presented as a linear combination of the above S (A)-type functions.

The Parametric Symmetrized Coordinates Representation

Now let us introduce the basis of orthonormalized eigenfunctions $\tilde{\Phi}_i(\boldsymbol{\xi};\xi_0)$, $\boldsymbol{\xi} = \{\xi_1,\ldots,\xi_{A-1}\}$ of a parametric $(A-1)$-dimensional oscillator with the energy eigenvalues $\tilde{\epsilon}_i(\xi_0)$:

$$\left[\sum_{i=1}^{A-1}\left(-\frac{\partial^2}{\partial\xi_i^2} + (\xi_i)^2\right) + U(\xi_0,\boldsymbol{\xi}\right) \qquad (21)$$

$$- \tilde{\epsilon}_i(\xi_0)\Big]\tilde{\Phi}_i(\boldsymbol{\xi};\xi_0) = 0,$$

$$U(\xi_0,\boldsymbol{\xi}) = \sum_{i,j=1;i<j}^{A} U^{\text{pair}}(x_{ij}(\boldsymbol{\xi})) + \sum_{i=1}^{A} V(x_i(\xi_0,\boldsymbol{\xi})).$$

We choose the parametric SCR (PSCR) basis functions as linear combinations of the S and A eigenfunctions $\Phi_{j'}^{S(A)}(\boldsymbol{\xi})$ constructed above:

$$\tilde{\Phi}_i(\boldsymbol{\xi};\xi_0) = \sum_{j'=1}^{j'_{\max}} \tilde{\alpha}_{j'}^{(i)}(\xi_0)\Phi_{j'}^{S(A)}(\boldsymbol{\xi}). \qquad (22)$$

Thus, the eigenvalue problem (21) is reduced to a parametric linearized version of the Hartree–Fock algebraic eigenvalue problem

$$\sum_{j'=1}^{j'_{\max}} (\delta_{ij'}E_i + U_{ij'}(\xi_0) \qquad (23)$$
$$- \delta_{ij'}\tilde{\epsilon}_i(\xi_0))\tilde{\alpha}_{j'}^{(i)}(\xi_0) = 0,$$
$$\sum_{j'=1}^{j'_{\max}} \tilde{\alpha}_{j'}^{(i')}(\xi_0)\tilde{\alpha}_{j'}^{(i)}(\xi_0) = \delta_{ii'},$$

where the effective potentials $U_{ij'}(\xi_0) = U_{ij'}^{\text{pair}} + V_{ij'}(\xi_0)$ are expressed in terms of the integrals

$$U_{ij'}^{\text{pair}} = \int d^{A-1}\boldsymbol{\xi}\Phi_i^{S(A)}(\boldsymbol{\xi}) \qquad (24)$$
$$\times \left(\sum_{k,k'=1;k<k'}^{A} U^{\text{pair}}(x_{kk'}(\boldsymbol{\xi}))\right)\Phi_{j'}^{S(A)}(\boldsymbol{\xi}),$$
$$V_{ij'}(\xi_0) = \int d^{A-1}\boldsymbol{\xi}\Phi_i^{S(A)}(\boldsymbol{\xi})$$
$$\times \left(\sum_{k=1}^{A} V(x_k(\xi_0,\boldsymbol{\xi}))\right)\Phi_{j'}^{S(A)}(\boldsymbol{\xi}).$$

Taking Eqs. (15) and (19) into account, integrals (24) are expressed via basis integrals

$$U_{ij}^{\text{pair}} \qquad (25)$$
$$= \sum_{i'[i''_1,\ldots,i''_{A-1}][j''_1,\ldots,j''_{A-1}]j'} \alpha_{ii'}^{S(A)}\beta_{i'[i''_1,\ldots,i''_{A-1}]}^{s(a)}$$
$$\times \bar{U}_{[i''_1,\ldots,i''_{A-1}][j''_1,\ldots,j''_{A-1}]}^{\text{pair}}\beta_{j'[i''_1,\ldots,i''_{A-1}]}^{s(a)}\alpha_{jj'}^{S(A)},$$
$$V_{ij}(\xi_0)$$
$$= \sum_{i'[i''_1,\ldots,i''_{A-1}][j''_1,\ldots,j''_{A-1}]j'} \alpha_{ii'}^{S(A)}\beta_{i'[i''_1,\ldots,i''_{A-1}]}^{s(a)}$$
$$\times \bar{V}_{[i''_1,\ldots,i''_{A-1}][j''_1,\ldots,j''_{A-1}]}(\xi_0)\beta_{j'[i''_1,\ldots,i''_{A-1}]}^{s(a)}\alpha_{jj'}^{S(A)},$$
$$\bar{U}_{[i''_1,\ldots,i''_{A-1}][j''_1,\ldots,j''_{A-1}]}^{\text{pair}} = \int d^{A-1}\boldsymbol{\xi}\bar{\Phi}_{[i''_1,\ldots,i''_{A-1}]}(\boldsymbol{\xi})$$
$$\times \left(\sum_{k,k'=1;k<k'}^{A} U^{\text{pair}}(x_{kk'}(\boldsymbol{\xi}))\right)\bar{\Phi}_{[j''_1,\ldots,j''_{A-1}]}(\boldsymbol{\xi}),$$
$$\bar{V}_{[i''_1,\ldots,i''_{A-1}][j''_1,\ldots,j''_{A-1}]}(\xi_0)$$
$$= \int d^{A-1}\boldsymbol{\xi}\bar{\Phi}_{[i''_1,\ldots,i''_{A-1}]}(\boldsymbol{\xi})$$
$$\times \left(\sum_{k=1}^{A} V(x_k(\xi_0,\boldsymbol{\xi}))\right)\bar{\Phi}_{[j''_1,\ldots,j''_{A-1}]}(\boldsymbol{\xi}).$$

If $U_{ij'}(\xi_0) = U_{ij'}^{\text{pair}}$ are independent of ξ_0, then $\tilde{\epsilon}_i(\xi_0) = \tilde{\epsilon}_i$ and $\tilde{\alpha}_{j'}^{(i)}(\xi_0) = \tilde{\alpha}_{j'}^{(i)}$ are also independent of ξ_0, and Eq. (22) reduces to

$$\tilde{\Phi}_i(\boldsymbol{\xi}) = \sum_{j'=1}^{j'_{\max}} \tilde{\alpha}_{j'}^{(i)}\Phi_{j'}^{S(A)}(\boldsymbol{\xi}). \qquad (26)$$

Moreover, if $U_{ij'}^{\text{pair}} = 0$, then $\tilde{\epsilon}_i = E_i^{S(A)}$ and $\tilde{\alpha}_{j'}^{(i)} = \delta_{ij'}$, and Eq. (26) reduces to Eq. (19). The solutions of the parametric eigenvalue problem (23) and their derivatives with respect to parameter ξ_0 are calculated by means of algorithms [50, 51].

An example of such parametric basis of S type at $A = 2$ was considered earlier [1, 18]. The case $A \geq 3$ will be considered elsewhere. The algebraic problem in symmetrized coordinates can be rewritten also in terms of the integrals that involve the eigenfunctions of $(A-1)$-dimensional harmonic oscillator in Jacobi coordinates, making use of the interbasis coefficients, generated by the transformations with $(A-1)$-dimensional *oscillator Wigner functions*, described in the previous subsection.

4. CLOSE-COUPLING EQUATIONS IN THE SCR

Now we proceed to seeking the solution of the problem (8) in the symmetrized coordinates in the form of Galerkin expansion

$$\Psi_{i_o}(\xi_0,\boldsymbol{\xi}) = \sum_{j=1}^{j_{\max}} \tilde{\Phi}_j(\boldsymbol{\xi})\chi_{ji_o}(\xi_0), \qquad (27)$$

where $\chi_i(\xi_0)$ are unknown functions

$$\chi_{ji_o}(\xi_0) = \int d^{A-1}\boldsymbol{\xi}\tilde{\Phi}_j(\boldsymbol{\xi})\Psi_{i_o}(\xi_0,\boldsymbol{\xi}),$$

and $\tilde{\Phi}_j(\boldsymbol{\xi})$ are the orthonormalized basis eigenfunctions (26) of the $(A-1)$-dimensional oscillator with

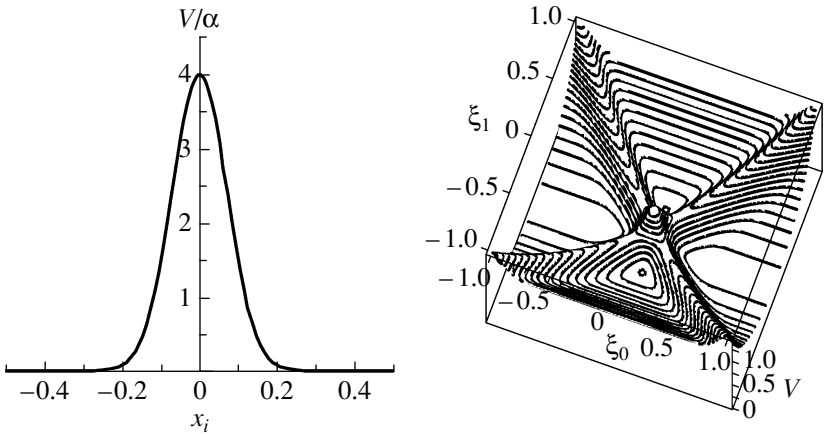

Fig. 8. (Left panel) Gaussian-type potential (30) at $\sigma = 0.1$ (in oscillator units). (Right panel) Corresponding 2D barrier potential at $\alpha = 1/10$, $\sigma = 0.1$.

the energy eigenvalues E_i, Eq. (14), constructed in the SCR.

The set of close-coupling Galerkin equations in the symmetrized coordinates has the form

$$\left[-\frac{d^2}{d\xi_0^2} + \tilde{\epsilon}_i - E\right]\chi_{ii_o}(\xi_0) + \sum_{j=1}^{j_{\max}} \tilde{V}_{ij}(\xi_0)\chi_{ji_o}(\xi_0) = 0, \tag{28}$$

where the effective potentials $\tilde{V}_{ij}(\xi_0)$ are calculated by means of $V_{ij}(\xi_0)$ from (24)

$$\tilde{V}_{ij}(\xi_0) = \sum_{j'=1}^{j'_{\max}} \sum_{j''=1}^{j'_{\max}} \tilde{\alpha}_{j'}^{(i)} V_{j'j''}(\xi_0)\tilde{\alpha}_{(j'')}^{(j)}, \tag{29}$$

and a set of the eigenvectors $\tilde{\alpha}_{j'}^{(i)}$ of the nonparametric algebraic problem (23) under the above condition $U_{ij'}(\xi_0) = U_{ij'}^{\text{pair}} \neq 0$. In the examples considered below we put $U_{ij'}(\xi_0) = U_{ij'}^{\text{pair}} = 0$ in (23), then we have $\tilde{\epsilon}_i = E_i^{S(A)}$, $\tilde{\alpha}_{j'}^{(i)} = \delta_{ij'}$ and $\tilde{V}_{ij}(\xi_0) = V_{ij}(\xi_0)$.

The repulsive barrier is chosen to be Gaussian

$$V(x_i) = \frac{\alpha}{\sqrt{2\pi}\sigma} \exp\left(-\frac{x_i^2}{\sigma^2}\right). \tag{30}$$

Figure 8 illustrates the Gaussian potential and the corresponding barrier potentials in symmetrized coordinates at $A = 2$. This potential has the oscillator-type shape, and two barriers are crossing at the right angle. In the case $A \geq 3$ the hyperplanes of barriers are crossing at the right angle, too. The effective potentials $V_{ij}(\xi_0)$ calculated using *symbolic algorithm SCR* described in the previous section are shown in Figs. 9 and 10. In comparison with the symmetric basis, for antisymmetric one the increase of the numbers i and/or j results in stronger oscillation of the effective potentials V_{ij} and weaker decrease of them to zero at $\xi_0 \to \infty$. At $A = 2$ all effective potentials are even functions, and at $A \geq 3$ some effective potentials are odd functions.

We can also seek for the solution of the problem (8) in symmetrized coordinates in the form of the Kantorovich expansion

$$\Psi_{i_o}(\xi_0, \boldsymbol{\xi}) = \sum_{j=1}^{j_{\max}} \tilde{\Phi}_j(\boldsymbol{\xi}; \xi_0)\tilde{\chi}_{ji_o}(\xi_0). \tag{31}$$

Here $\tilde{\chi}_{ii_o}(\xi_0)$ are unknown functions

$$\tilde{\chi}_{ji_o}(\xi_0) = \int d^{A-1}\boldsymbol{\xi}\tilde{\Phi}_j(\boldsymbol{\xi}; \xi_0)\Psi_{i_o}(\xi_0, \boldsymbol{\xi}),$$

and $\tilde{\Phi}_i(\boldsymbol{\xi}; \xi_0)$ are the orthonormalized basis eigenfunctions of the parametric $(A-1)$-dimensional oscillator with eigenenergies $\tilde{E}_i(\xi_0)$ from Eq. (21) in the PSCR. Taking Eqs. (15) and (13) into account, the set of the close-coupling equations in the Kantorovich form reads as

$$\left[-\frac{d^2}{d\xi_0^2} + \tilde{\epsilon}_i(\xi_0) - E\right]\tilde{\chi}_{ii_o}(\xi_0) + \sum_{j=1}^{j_{\max}} \left[H_{ij}(\xi_0) + \frac{d}{d\xi_0}Q_{ij}(\xi_0) + Q_{ij}(\xi_0)\frac{d}{d\xi_0}\right] \times \tilde{\chi}_{ji_o}(\xi_0) = 0, \tag{32}$$

where the effective potentials $H_{ij}(\xi_0)$ and $Q_{ij}(\xi_0)$ are calculated

$$H_{ij}(\xi_0) = \sum_{j'=1}^{j'_{\max}} \frac{d\tilde{\alpha}_{j'}^{(i)}(\xi_0)}{d\xi_0} \frac{d\tilde{\alpha}_{j'}^{(j)}(\xi_0)}{d\xi_0}, \tag{33}$$

Table 5. The degeneracy multiplicities p from (16), $p_s = p_a$ and $p_S = p_A$ of s, a, S, and A eigenfunctions of the oscillator energy levels $\Delta E_j = E_j^\bullet - E_1^\bullet$ ($\bullet = 0, s, a, S, A$)

$A=3$			$A=4$			$A=5$			$A=6$			ΔE_j
p	p_s, p_a	p_S, p_A	p	p_s, p_a	p_S, p_A	p	p_s, p_a	p_S, p_A	p	p_s, p_a	p_S, p_A	
1	1	1	1	1	1	1	1	1	1	1	1	0
2	1	0	3	1	0	4	1	0	5	1	0	2
3	2	1	6	2	1	10	2	1	15	2	1	4
4	2	1	10	3	1	20	3	1	35	3	1	6
5	3	1	15	4	2	35	5	2	70	5	2	8
6	3	1	21	5	1	56	6	2	126	7	2	10
7	4	2	28	7	3	84	9	3	210	10	4	12

Table 6. Resonance values of the energy E_S (E_A) (in oscillator units) for S (A) states for $A = 2, 3, 4$ ($\sigma = 1/10, \alpha = 20$) with approximate eigenvalues E_i^D, for the first ten states $i = 1, \ldots, 10$, calculated using the truncated oscillator basis (D) till $j_{\max} = 136, 816, 1820$ at $A = 2, 3, 4$

i	1	2	3	4	5	6	7	8	9	10
					$A=2$					
E_S	5.72	9.06	9.48	12.46	12.57	13.46	15.74	15.78	16.65	17.41
E_A	5.71	9.06	9.48	12.45	12.57	13.45	15.76*	15.76*	16.66	17.40
E_i^D	5.76	9.12	9.53	12.52	12.64	13.52	15.81	15.84	16.73	17.47
					$A=3$					
E_S	8.18	11.11		12.60	13.93		14.84	15.79		16.67
	8.31	11.23			14.00		14.88			16.73
E_A			11.55			14.46			16.18	
			11.61			14.56			16.25	
E_i^D	8.19	11.09	11.52	12.51	13.86	14.42	14.74	15.67	16.11	16.53
					$A=4$					
E_S	10.12	11.89	12.71	14.86	15.19	15.41	15.86	16.37	17.54	17.76
E_i^{D31}	10.03		12.60	14.71	15.04			16.18	17.34	17.56
E_i^{D22}		11.76				15.21	15.64			

* Two overlapping peaks of transmission probability.

$$Q_{ij}(\xi_0) = -\sum_{j'=1}^{j'_{\max}} \tilde{\alpha}_{j'}^{(i)}(\xi_0) \frac{d\tilde{\alpha}_{j'}^{(j)}(\xi_0)}{d\xi_0},$$

using the solutions $\tilde{\epsilon}_i(\xi_0)$ and $\tilde{\alpha}_{j'}^{(i)}(\xi_0)$, and their first derivatives of the parametric algebraic eigenvalue problem (23). Note, that the PSCR constructed in the above form with the long derivative $D_{ij} = \delta_{ij} d/d\xi_0 - Q_{ij}(\xi_0)$ can be treated as *an alternative version* [52] of the method of generator coordinates with velocity-dependent effective potential [53, 54]. Indeed, equations (32) can be rewritten in the terms of long derivatives D_{ij}, which apply in some adiabatic calculations

$$\sum_{j=1}^{j_{\max}} \left[-D_{ij}^2 + \mathcal{F}_{ij}(\xi_0) + (\tilde{\epsilon}_i(\xi_0) - E)\delta_{ij} \right] \times \tilde{\tilde{\chi}}_{ji_o}(\xi_0) = 0. \quad (34)$$

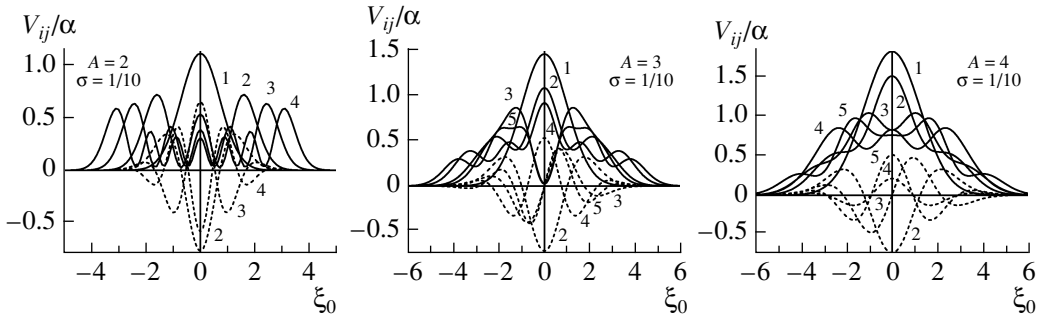

Fig. 9. Diagonal V_{jj} (solid lines) and nondiagonal V_{j1} (dashed lines) effective potentials for $A = 2$, $A = 3$, and $A = 4$ of the S states of the particles at $\sigma = 0.1$. j is the number of the state in Table 3.

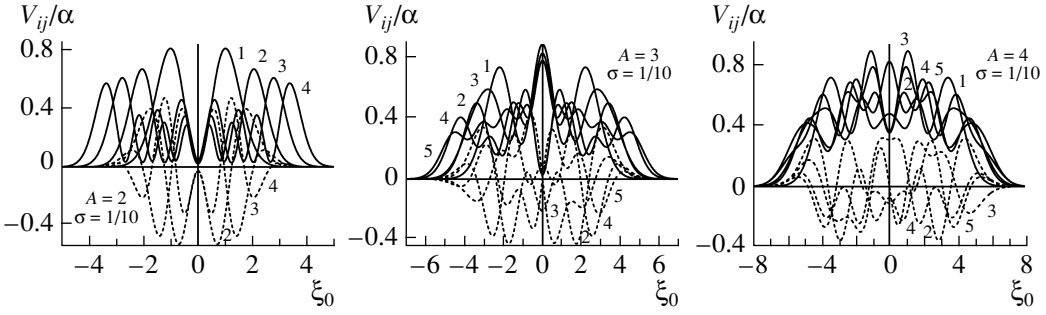

Fig. 10. The same as in Fig. 9 but for A states. j is the number of state in Table 4.

However, the curvature matrix elements

$$\mathcal{F}_{ij}(\xi_0) = H_{ij}(\xi_0) - \sum_{j''=1}^{j''_{\max}} Q_{ij''}(\xi_0)Q_{j''j}(\xi_0)$$

tend to zero only at $j''_{\max} \gg j'_{\max} \gg j_{\max}$. This fact explains the different rate of convergence of approximate solutions to exact ones with increasing $j_{\max}$ in different calculations. The asymptotic form of the matrix solution $\tilde{\chi}_{ji_o}(\xi_0)$, compatible with (9), was derived earlier in [18].

Thus, the scattering problem (8) with the asymptotic boundary conditions (9) is reduced to the boundary-value problem for the set of close-coupling equations in Galerkin or Kantorovich form, (28) or (32), with the boundary conditions at $d = 1$, $\xi_0 = \xi_{\min}$ and $\xi_0 = \xi_{\max}$:

$$\left.\frac{d\mathbf{F}(\xi_0)}{d\xi_0}\right|_{\xi_0=\xi_{\min}} = \mathcal{R}(\xi_{\min})\mathbf{F}(\xi_{\min}), \qquad (35)$$

$$\left.\frac{d\mathbf{F}(\xi_0)}{d\xi_0}\right|_{\xi_0=\xi_{\max}} = \mathcal{R}(\xi_{\max})\mathbf{F}(\xi_{\max}),$$

where $\mathcal{R}(\xi)$ is an unknown $j_{\max} \times j_{\max}$ matrix function, $\mathbf{F}(\xi_0) = \{\boldsymbol{\chi}_{i_o}(\xi_0)\}_{i_o=1}^{N_o} = \{\{\chi_{ji_o}(\xi_0)\}_{j=1}^{j_{\max}}\}_{i_o=1}^{N_o}$ is the required $j_{\max} \times N_o$ matrix solution, and N_o is the number of open channels, $N_o = \max\limits_{2E \geq E_j} j \leq j_{\max}$, calculated using the third version of KANTBP program [55], described in [18, 41].

5. RESONANCE TRANSMISSION OF A FEW COUPLED PARTICLES

In the case of $V^{\text{pair}}(x_{ij}) = V^{\text{hosc}}(x_{ij})$, the solution of the scattering problem described above yields the reflection and transmission amplitudes $R_{ji_o}(E)$ and $T_{ji_o}(E)$ that enter the asymptotic boundary conditions (9) as unknowns. $|R_{ji_o}(E)|^2$ ($|T_{ji_o}(E)|^2$) is the probability of a transition to the state, described by the reflected (transmitted) wave and, hence, will be referred as the reflection (transmission) coefficient. Note that $|R_{ji_o}(E)|^2 + |T_{ji_o}(E)|^2 = 1$.

In Figs. 11, 12, and 13 we show the energy dependence of the total transmission probability $|T|^2_{ii} = \sum_{j=1}^{N_o} |T_{ji}(E)|^2$. This is the probability of a transition from a chosen state i into any of N_o states, found from Eq. (27) by solving the boundary-value problem in the Galerkin form, (28) and (35), with the KANTBP program [55] on the finite-element grid $\Omega_\xi\{-\xi_0^{\max}, \xi_0^{\max}\}$ with N_{elem} fourth-order Lagrange elements between the nodes. For S solutions at $N = 2, 3, 4$ the following parameters are used: $j_{\max} = 13, 21, 39$, $\xi_0^{\max} = 9.3, 10.5, 12.8$, $N_{\text{elem}} = 664, 800, 976$, while for A solutions $j_{\max} = 13, 16, 15$, $\xi_0^{\max} = 9.3, 10.5, 12.2$,

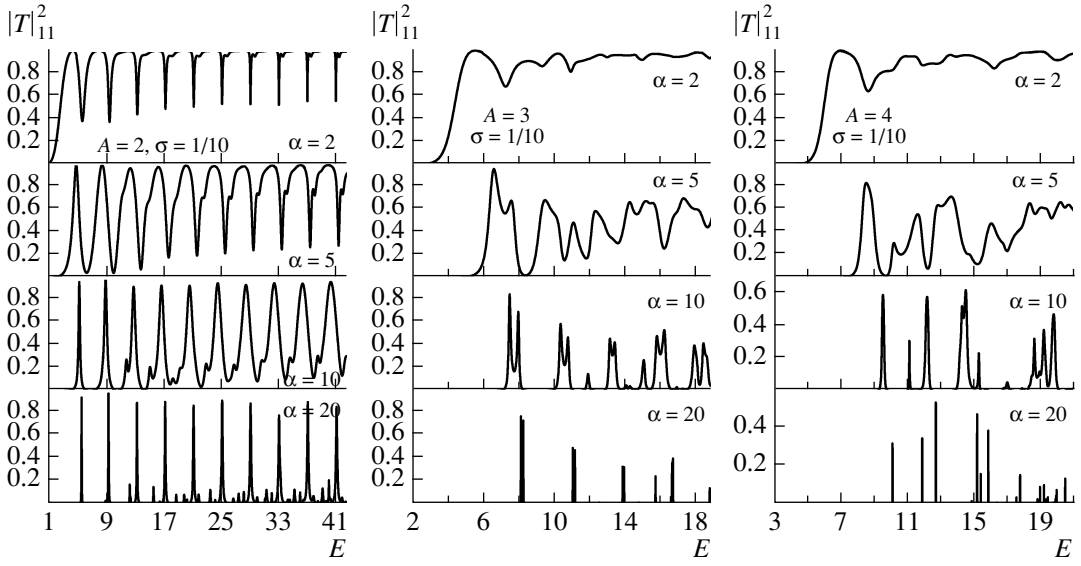

Fig. 11. The total transmission probabilities $|T|^2_{11}$ vs energy E (in oscillator units) from the ground state of the system of $A = 2, 3, 4$ of the S states of the particles, coupled by the oscillator potential, through the repulsive Gaussian-type potential barriers (30) at $\sigma = 0.1$ and $\alpha = 2, 5, 10, 20$.

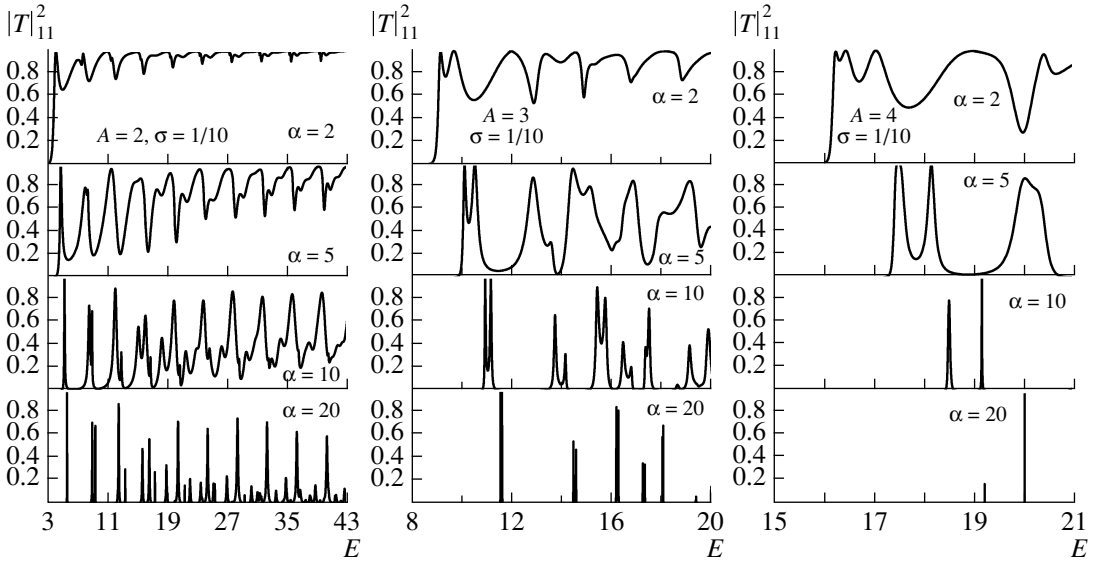

Fig. 12. The same as in Fig. 11 but for A states of the particles.

$N_{\text{elem}} = 664, 800, 976$. Figures 11 and 12 demonstrate the nonmonotonic behavior of the probability versus the energy, and the observed resonances are manifestations of the quantum transparency effect. With the barrier height increasing, the peaks become narrower and their positions shift to higher energies. The multiplet structure of the peaks in the symmetric case is similar to that in the antisymmetric case. For three particles the major peaks are double, while for two and four particles they are single. For $A = 2$ and $\alpha = 10, 20$ one can observe additional multiplets of small peaks. Figure 13 illustrates the energy dependence of transmission probabilities from the exited states. As the energy of the initial excited state increases, the transmission peaks demonstrate a shift towards higher energies, the set of peak positions keeping approximately the same as for the transitions from the ground state and the peaks just changing one position for another, like it was observed in the model calculations [14]. For example, for $A = 3$ the position of the third peak for transitions from the first two states ($E = 10.4167$ and $E = 10.4156$)

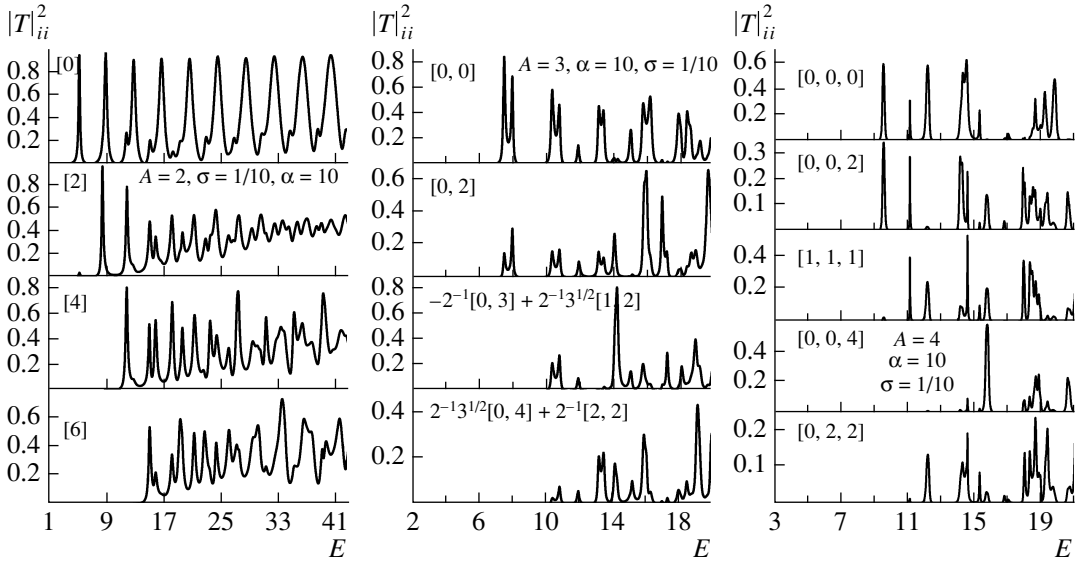

Fig. 13. The total penetration probabilities $|T|^2_{ii}$ vs energy E (in oscillator units) from the ground and excited states of the system of $A = 2, 3, 4$ of the S states of the particles, coupled by the oscillator potential, through the repulsive Gaussian-type potential barriers (30) at $\sigma = 0.1$ and $\alpha = 10$.

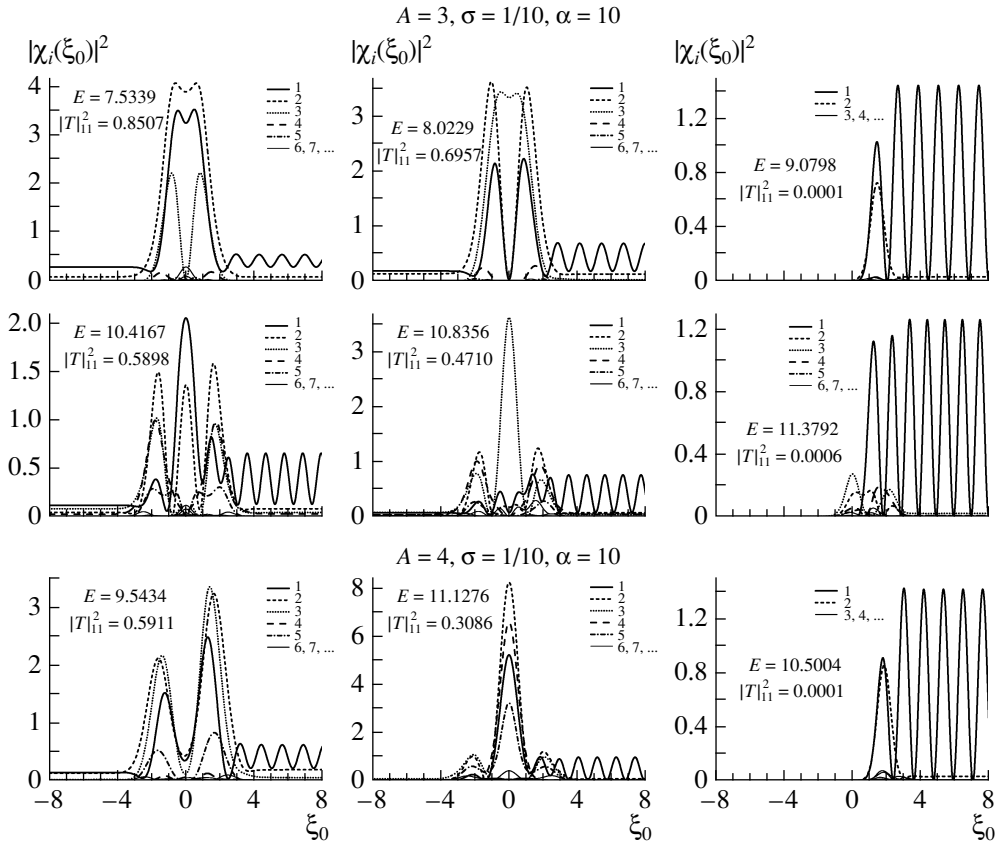

Fig. 14. The probability densities $|\chi_i(\xi_0)|^2$ of coefficient functions of decomposition (27), representing the incident wave function of the ground S state of the particles at the values of the collision energy E, corresponding to some maxima and minima of the transmission coefficient in Fig. 11 for the parameters of the Gaussian barrier $\alpha = 10$ and $\sigma = 0.1$.

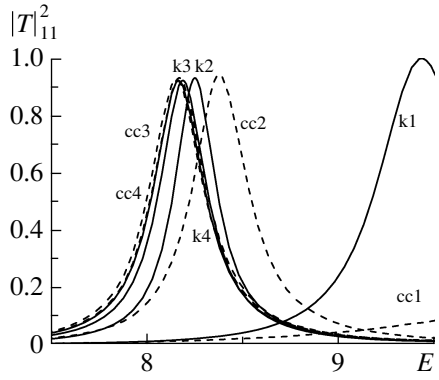

Fig. 15. The epures of the first peak in Fig. 11 illustrating the convergence of Galerkin (cc*) and Kantorovich (k*) close-coupling expansions in calculations of transmission coefficient $|T|^2_{11}$ for the S-states, $A = 2$ at $\alpha = 10$, $\sigma = 0.1$ (E in oscillator units).

coincides with the position of the first peak for the transitions from the second two states ($E = 10.4197$ and $E = 10.4298$).

The effect of quantum transparency is caused by the existence of barrier quasistationary states, embedded in the continuum. Figure 14 shows that in the case of resonance transmission the wave functions, depending on the center-of-mass variable ξ_0, are localized in the vicinity of the potential barrier center ($\xi_0 = 0$).

For the energy values, corresponding to some of the transmission coefficient peaks in Fig. 11 at $\alpha = 10$ within the effective range of barrier potential action, the wave functions demonstrate considerable increase (from two to ten times) of the probability density in comparison with the incident unit flux. This is a fingerprint of quasistationary states, which is not a quantitative definition, but a clear evidence in favor of their presence in the system [56, 57].

In the case of total reflection the wave functions are localized at the barrier side, on which the wave is incident, and decrease to zero within the effective range of the barrier action.

Note that the explicit explanation of quantum transparency effect is achieved in the frame of Kantorovich close-coupling equations (32) because of the multi-barrier potential structure of the effective potential (33), appearing explicitly even in the diagonal or adiabatic approximation, in particular, in the S case for $A = 2$ [1, 18]. Nevertheless, in Galerkin close-coupling equations the multi-barrier potential structure of the effective potential is observed explicitly in the A case (see Fig. 10).

As an example, Fig. 15, which is an epure of Fig. 11, shows the comparison of convergence rates of Galerkin (27) and Kantorovich (31) close-coupling expansions in calculations of transmission coefficient $|T|^2_{11}$ for S wave functions, $A = 2$ at $\alpha = 10$, $\sigma = 0.1$. One can see that the diagonal approximation of the Kantorovich method provides better approximations of the positions of the transmission coefficient $|T|^2_{11}$ resonance peaks. With the increasing number of basis functions, i.e., the number $j_{\max}$ of close-coupling equations with respect to the center-of-mass coordinates in Galerkin (28) and Kantorovich (32) form, respectively, the convergence rates are similar and confirm the results obtained by solving the problem by means of the Finite-Difference Numerov method in 2D domain [1]. This is true for the considered short-range potentials (30), while for long-range potentials of the Coulomb type the Kantorovich method can be more efficient [18].

Figure 16 shows the profiles of $|\Psi|^2 \equiv |\Psi^{(-)}_{Em\rightarrow}|^2$ for the S and A total wave functions of the continuous spectrum in the (ξ_0, ξ_1) plane with $A = 2$, $\alpha = 10$, $\sigma = 1/10$ at the resonance energies of the first and the second maximum and the first minimum of the transmission coefficient demonstrating *resonance transmission* and *total reflection*, respectively. It is seen that in the case of resonance transmission the redistribution of energy from the center-of-mass degree of freedom to the internal (transverse) ones takes place, i.e., the transverse oscillator undergoes a transition from the ground state to the excited state, while in the total reflection the redistribution of energy is extremely small and the transverse oscillator returns to infinity in the same state.

In Table 6 we present the resonance values of the energy E_S (E_A) calculated by solving the boundary-value problem (28) and (35), using the KANTBP 3.0 program, for S (A) states at $A = 2, 3, 4$, $\sigma = 1/10$, $\alpha = 20$ that correspond to the maxima of transmission coefficients $|T|^2_{ii}$ in Fig. 11 up to the values of energy $E < 18$ and the corresponding resonance values of the energy E_D calculated by means of the Dirichlet conditions (DC) algorithm. One can see, that the accepted approximation of narrow barrier with impermeable walls using in the DC algorithm provides an appropriate approximation E^D_i of the above high accuracy results E_S (E_A) with the error smaller than 2%. Below we give a comparison and qualitative analysis of the obtained results.

In the considered case the potential barrier $V(x_i)$ is narrow and $V^{\text{pair}}(x_{ij}) = V^{\text{hosc}}(x_{ij})$, so that we solve Eq. (1) in the Cartesian coordinates $x_1, \ldots, x_A$ in one of the 2^A-2 subdomains, defined as $p_i x_i > 0$, $p_i = \pm 1$, with the DC: $\Psi(x_1, \ldots, x_A)|_{\cup^A_{i=1}\{x_i=0\}} = 0$ at the internal boundaries $\cup^A_{i=1}\{x_i = 0\}$. Here, the value $p_i = \pm 1$ indicates the location of the ith particle at the right or left side of the barrier, respectively. Thus, in the DC procedure we seek for the solution in

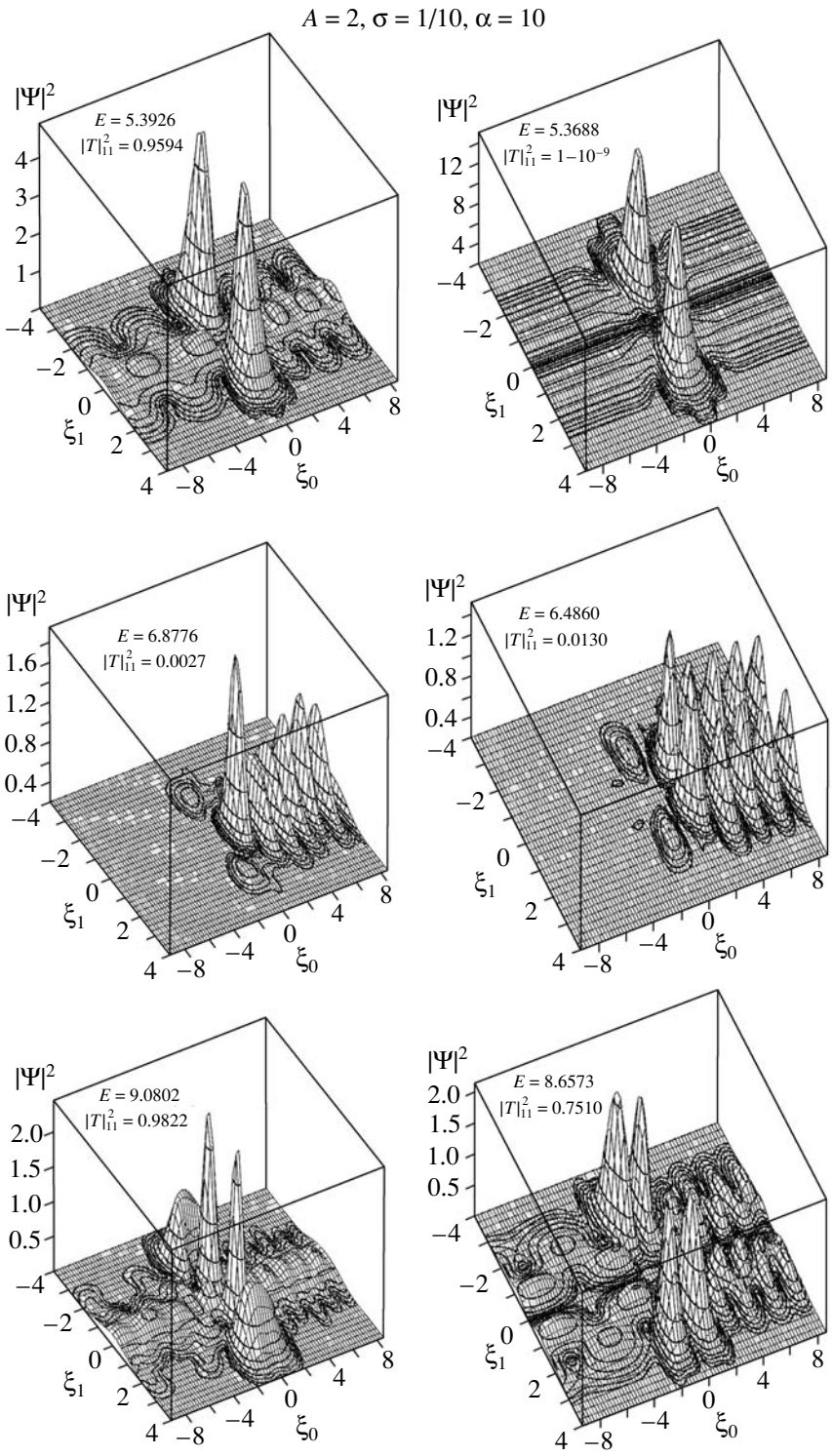

Fig. 16. The profiles of probability densities $|\Psi(\xi_0, \xi_1)|^2$ for the S (left panels) and A (right panels) states of $A = 2$ particles, revealing resonance transmission and total reflection at resonance energies, depicted in Figs. 11 and 12.

the form of a Galerkin expansion over the orthogonal truncated oscillator basis, $\Psi_i^D(\mathbf{x}) = \sum_{j=1}^{j_{\max}} \bar{\Phi}_j(\mathbf{x})\Psi_{ji}^D$ composed of A-dimensional harmonic oscillator functions $\bar{\Phi}_j(\mathbf{x})$, odd in each of the Cartesian coordinates $x_1, \ldots, x_A$ in accordance with the above DCs, with unknown coefficients Ψ_{ji}^D. As a result, we arrive at the algebraic eigenvalue problem $\mathbf{D}\boldsymbol{\Psi}^{\mathbf{D}} = \boldsymbol{\Psi}^{\mathbf{D}}\mathbf{E}^{\mathbf{D}}$ with a dense real-symmetric $j_{\max} \times j_{\max}$ matrix. So,

in the DC procedure we seek for an approximate solution in one of the potential wells, i.e., we neglect the tunnelling through the barriers between wells. Therefore, we cannot observe the splitting, inherent in exact eigenvalues, corresponding to S and A eigenstates, differing in permutation symmetry. However, we can explain the mechanism of their appearance and give their classification, which is important, too. The DC algorithm was implemented in CAS Maple and Fortran environment and published in [58].

Remark. The DC procedure is similar to solving Eq. (8) in the symmetrized coordinates $\xi_0, \boldsymbol{\xi}$ related to the Cartesian ones via Eq. (3), implemented by the following two steps:

(i) we approximate the narrow barriers by impenetrable walls $x_k(\xi_0, \boldsymbol{\xi}) = 0$;

(ii) we superpose these mutually perpendicular walls with the coordinate hyperplanes using rotations.

Actually, the two approaches yield the same boundary-value problem, formulated in different coordinates (1), (8).

Below we give a comparison and qualitative analysis of the obtained results. For two particles, $A = 2$ (see Fig. 8), there are two symmetric potential wells. In each of them both symmetric and asymmetric wave functions are constructed. Since the potential barrier, separating the wells, is sufficiently high, the appropriate energies are closely spaced, so that each level describes the states of both S and A type. The lower energy levels form a sequence "singlet–doublet–triplet, etc.", which is seen in Fig. 11. The resonance transmission energies for a pair of particles in S states is lower than that for a pair of those in A states. This is due to the fact that in the vicinity of the collision point the wave function is zero.

When $A = 3$, there are six similar wells, three of them at each side of the plane $\xi_0 = 0$. The symmetry with respect to the plane $\xi_0 = 0$ explains the presence of doublets. The presence of states with definite symmetry is associated with the fact that the axis ξ_0 is a third-order symmetry axis. However, in contrast to the case $A = 2$, one can obtain either S or A combinations of states. For example, the first four solutions of the problem, in one of the wells (e.g., the one restricted with the pair-collision planes "13" and "23") possess the dominant components $2\sqrt{2}\bar{\Phi}_1(x_1)\bar{\Phi}_1(x_2)\bar{\Phi}_1(x_3)$, $2(\bar{\Phi}_1(x_1)\bar{\Phi}_3(x_2) + \bar{\Phi}_3(x_1)\bar{\Phi}_1(x_2))\bar{\Phi}_1(x_3)$, $2(\bar{\Phi}_1(x_1)\bar{\Phi}_3(x_2) - \bar{\Phi}_3(x_1) \times \Phi_1(x_2))\bar{\Phi}_1(x_3)$, $2\sqrt{2}\bar{\Phi}_1(x_1)\bar{\Phi}_1(x_2)\bar{\Phi}_3(x_3)$. Note, that the first, second, and fourth of these functions are symmetric with respect to the permutation $x_1 \leftrightarrow x_2$, while the third one is antisymmetric. Hence, in all six wells using the first four solutions one can obtain six S and two A states.

When $A = 4$ there are 14 wells. Six wells in the center correspond to the case when two particles are located at one side of the barrier and the rest two at the other side. The corresponding eigenenergy is denoted as E_i^{D22}. The rest eight wells correspond to the case when one particle is located at one side of the barrier and the rest three at the other side. The corresponding eigenenergy is denoted as E_i^{D31}. For these states doublets must be observed, similar to the case of three particles. However, the separation between the energy levels is much smaller, because the 4-well groups are strongly separated by two barriers, instead of only one barrier in the case $A = 3$.

The necessary condition for the quasi-stationary state being symmetric (antisymmetric) is that the wave functions must be symmetric (antisymmetric) with respect to those coordinates x_i and x_j, for which $p_i = p_j$.

6. CONCLUSION

We considered a model of A identical particles bound by the oscillator-type potential that undergo quantum tunnelling through the short-range repulsive barrier potentials. The model was formulated in the new representation, which we referred as symmetrized coordinate representation (SCR). The constructive method of symmetrizing or antisymmetrizing the harmonic oscillator basis functions in the new symmetrized coordinates was described. We had shown that the transformations of $(A-1)$-dimensional oscillator basis functions from the symmetrized coordinates to the Jacobi coordinates, reducible to permutations of coordinates and $(A-1)$-dimensional finite rotation, are implemented by means of the $(A-1)$-dimensional *oscillator Wigner functions* [45], while the reduction of the SCR in the Cartesian coordinates to the hyperspherical ones is given by means of the *Clebsch–Gordan coefficients of the interbasis expansions* [47]. One can use the above transformations to recalculate the SCR, $(A-1)$-harmonic oscillator functions of symmetric or antisymmetric type with respect to permutations of Cartesian coordinates of A identical particles, in desirable sets of Jacobi and/or hyperspherical coordinates.

For clarity a system of several identical particles in one-dimensional Euclidean space ($d = 1$) was considered with a discrete spectrum of relative motion in the center-of-mass coordinate system, described by the internal symmetrized variables, and a continuous spectrum of the center-of-mass motion, described by the external variable. We calculated only the spatial part of the wave function, symmetric or antisymmetric under permutation of A identical particles. If

necessary, the spin part of the wave function can be determined using the conventional procedure and included in a more rigorous calculation.

The multichannel scattering problem for the Schrödinger equation with several short-range repulsive barriers was formulated. The problem was reduced to the boundary-value problem for a set of the close-coupling second-order differential equations with respect to the longitudinal variable on the whole axis. This was implemented by expanding the wave function over the oscillator basis of several bound particles possessing symmetry or antisymmetry under permutations of A initial Cartesian coordinates.

We analyzed the effect of quantum transparency, i.e., the resonance tunnelling of several bound particles through repulsive potential barriers. We demonstrated that this effect is due to the existence of the sub-barrier quasi-stationary states, embedded in the continuum. For the considered type of symmetric Gaussian barrier potential the positions of the energies of the S and A quasi-stationary states have a small difference, because of the similar multiplet structure of oscillator energy levels at a fixed number of particles. This fact explains the similar behavior of transmission coefficients from S and A states shifted by the threshold energies. However, the multiplet structure of energy positions of these states is varied with increasing number of particles such that for three particles the major peaks are double, while for two and four particles they are single. Our calculations also show that with the increasing energy of the initial excited state of few-body clusters, the transmission peaks demonstrate a shift towards higher energies, the set of peak positions keeping approximately the same as for the transitions from the ground state and the peaks just skipping from one position for another.

The proposed approach can be adapted and applied to the analysis of tetrahedral-symmetric nuclei, the study of quantum diffusion of molecules and micro-clusters through surfaces and the fragmentation mechanism in producing very neutron-rich light nuclei. In connection with the intense search for superheavy nuclei, a particularly significant application of the proposed approach is the mathematically correct analysis of mechanisms of sub-barrier fusion of heavy nuclei and the study of fusion rate enhancement by means of resonance tunnelling.

The authors thank Profs. A. Amaya Tapia, V.B. Belyaev, A. Dobrowolski, S.N. Ershov, V.P. Gerdt, G.P. Kamuntavičius, F.M. Pen'kov, G.S. Pogosyan, and V.V. Pupyshev for useful discussions. The work was supported partially by grants nos. 13-602-02 JINR, 11-01-00523 and 13-01-00668 RFBR, 0602/GF MES RK and the Bogoliubov–Infeld program.

REFERENCES

1. F. M. Pen'kov, J. Exp. Theor. Phys. **91**, 698 (2000); Phys. Rev. A **62**, 044701 (2000).
2. T. Sato and Y. Kayanuma, Europhys. Lett. **60**, 331 (2002).
3. E. Pijper and A. Fasolino, J. Chem. Phys. **126**, 014708 (2007).
4. D. I. Bondar, W.-Ki Liu, and M. Yu. Ivanov, Phys. Rev. A **82**, 052112 (2010).
5. M. R. A. Shegelski et al., Eur. Phys. J. Plus **127**, 17 (2012).
6. S. N. Ershov and B. V. Danilin, Phys. Part. Nucl. **39**, 835 (2008).
7. P. Navrátil, G. P. Kamuntavičius, and B. R. Barrett, Phys. Rev. C **61**, 044001 (2000).
8. B. E. Grinyuk and I. V. Simenog, Phys. At. Nucl. **72**, 6 (2009).
9. A. V. Nesterov et al., Phys. Part. Nucl. **41**, 716 (2010).
10. H. Hofmann, Nucl. Phys. A **224**, 116 (1974).
11. H. J. Krappe et al., Z. Phys. A **314**, 23 (1983).
12. K. Hagino, N. Rowley, and A. T. Kruppa, Comput. Phys. Commun. **123**, 143 (1999).
13. V. I. Zagrebaev and V. V. Samarin, Phys. At. Nucl. **67**, 1462 (2004).
14. N. Ahsan and A. Volya, Phys. Rev. C **82**, 064607 (2010).
15. A. C. Shotter and M. D. Shotter, Phys. Rev. C **83**, 054621 (2011).
16. V. M. Shilov, Phys. At. Nucl. **75**, 449 (2012).
17. O. Chuluunbaatar et al., Phys. At. Nucl. **72**, 768 (2009).
18. A. A. Gusev et al., Lect. Notes Comp. Sci. **6885**, 175 (2011).
19. M. Dobrowolski et al., Int. J. Mod. Phys. E **20**, 500 (2011).
20. Sh. Tagami, Yo. R. Shimizu, and J. Dudek, arXiv:1301.3279v1 [nucl-th].
21. Yo. Kanada-En'yo and Yo. Hidaka, Phys. Rev. C **84**, 014313 (2011).
22. V. A. Fock, Z. Phys. **61**, 126 (1930); Usp. Fiz. Nauk **93**, 342 (1967); *Fundamentals of Quantum Mechanics* (Mir, Moscow, 1978) [in Russian].
23. M. Hamermesh, *Group Theory and Its Application to Physical Problems* (Dover, 1989).
24. C. Lubich, *From Quantum to Classical Molecular Dynamics: Reduced Models and Numerical Analysis* (European Mathematical Society Publ., Zürich, 2008).
25. L. V. Kantorovich and V. I. Krylov, *Approximate Methods of Higher Analysis* (Wiley, New York, 1964).
26. P. Kramer and M. Moshinsky, Nucl. Phys. **82**, 241 (1966).
27. M. Kretzschmar, Z. Phys. **157**, 433, 558 (1960); Z. Phys. **158**, 284 (1960).
28. V. G. Neudatchin and Yu. F. Smirnov, *Nucleon Clusters in the Light Nuclei* (Nauka, Moscow, 1969) [in Russian].

29. M. Moshinsky and Y. F. Smirnov, *The Harmonic Oscillator in Modern Physics* (Informa Health Care, Amsterdam, 1996).
30. K. Wildermuth and Y. C. Tang, *A Unified Theory of the Nucleus* (Vieweg, Braunschweig, 1977).
31. A. Novoselsky and J. Katriel, Ann. Phys. (N.Y.) **196**, 135 (1989).
32. G. P. Kamuntavičius, Few-Body Syst. **1**, 91 (1986).
33. G. Kamuntavičius, Sov. J. Part. Nucl. **20**, 109 (1989); A. Deveikis and G. Kamuntavičius, Lithuanian Phys. J. **37**, 371 (1997).
34. V. V. Pupyshev, Phys. Part. Nucl. **30**, 689 (1999).
35. V. V. Kornyak, Phys. At. Nucl. **76**, 240 (2013); arXiv:1208.5734.
36. G. P. Kamuntavičius et al., Nucl. Phys. A **695**, 191 (2001).
37. V. C. Aguilera-Navarro, M. Moshinsky, and W. W. Yeh, Ann. Phys. (N.Y.) **51**, 312 (1969); V. C. Aguilera-Navarro, M. Moshinsky, and P. Kramer, Ann. Phys. (N.Y.) **54**, 379 (1969); J.-M. Lévy-Leblond, J. Math. Phys. **7**, 2217 (1966).
38. D. W. Jepsent and J. O. Hirschfelder, Proc. Natl. Acad. Sci. USA **45**, 249 (1959); J. O. Hirschfelder, Int. J. Quantum Chem. **3** (Suppl. S3a), 17 (1969).
39. R. T. Pack and G. A. Parker, J. Chem. Phys. **87**, 3888 (1987).
40. V. S. Buslaev et al.,Phys. At. Nucl. **76**, 208 (2013).
41. A. A. Gusev, O. Chuluunbaatar, and S. I. Vinitsky, in *Proceedings of the 2nd International Conference on The Modeling of Non-Linear Processes and Systems*, Ed. L. A. Uvarova (Yanus, Moscow, 2011).
42. M. Abramowitz and I. A. Stegun, *Handbook of Mathematical Functions* (Dover, New York, 1965).
43. G. A. Baker, Jr., Phys. Rev. **103**, 1119 (1956).
44. A. Gusev et al., Lect. Notes Comp. Sci. (accepted).
45. G. S. Pogosyan, Ya. A. Smorodinsky, and V. M. Ter-Antonyan, J. Phys. A **14**, 769 (1981).
46. D. A. Varshalovich, A. N. Moskalev, and V. K. Chersonsky, *Quantum Theory of Angular Momentum: Irreducible Tensors, Spherical Harmonics, Vector Coupling Coefficients, 3nj Symbols* (Nauka, Leningrad, 1975; World Scienrific, Singapore, 1988).
47. L. G. Mardoyan, G. S. Pogosyan, A. N. Sissakyan, and V. M. Ter-Antonyan, *Quantum System with Hidden Symmetry. Interbasis Expansion* (Fizmatlit, Moscow, 2006) [in Russian].
48. J. M. Lévy-Leblond, Phys. Lett. A **26**, 540 (1968).
49. Zh. Wang et al., arXiv:1108.1607v4 [math-ph].
50. S. I. Vinitsky, V. P. Gerdt, A. A. Gusev, et al., Progr. Computer Software **33**, 105 (2007).
51. C. F. Bunge, Comput. Phys. Commun. **138**, 92 (2001).
52. V. M. Dubovik et al., Bulgarian J. Phys. **17**, 1 (1990).
53. J. J. Griffin and J. A. Wheeler, Phys. Rev. **108**, 311 (1957).
54. D. Baye, P.-H. Heenen, and M. Libert-Heinemann, Nucl. Phys. A **291**, 230 (1977).
55. O. Chuluunbaatar et al., Comput. Phys. Commun. **179**, 685 (2008).
56. A. I. Baz', Ya. B. Zel'dovich, and A. M. Perelomov, *Scattering, Reactions, and Decay in Nonrelativistic Quantum Mechanics* (Jerusalem, 1969; Nauka, Moscow, 1971).
57. C. A. A. de Carvalho and H. M. Nussenzveig, Phys. Rep. **364**, 83 (2002).
58. S. Vinitsky et al., Lect. Notes Comp. Sci. (accepted).